Enzymes in Bacterial Amine Degradation: Biochemical and Electrochemical Characterization of Quinohemoprotein Amine Dehydrogenase and Histamine Dehydrogenase

Nobutaka Fujieda

2006

Enzymes in Bacterial Amine Degradation: Biochemical and Electrochemical Characterization of Quinohemoprotein Amine Dehydrogenase and Histamine Dehydrogenase

Nobutaka Fujieda

2006

CONTENTS

Abbreviations: MADH, methylamine dehydrogenase; QH-AmDH, quinohemoprotein amine dehydrogenase; *s*QH-AmDH, silent form quinohemoprotein amine dehydrogenase; HmDH, histamine dehydrogenase; TMADH, trimethylamine dehydrogenase; DMADH, dimethylamine dehydrogenase; ETF, electron transfer flavoprotein; TTQ, tryptophan tryptophylquinone; CTQ, cysteine tryptophylquinone; LTQ, lysine tyrosylquinone; TPQ, topa quinone; *P. denitrificans, Paracoccus denitrificans*; *N. simplex, Nocardioides simplex*; FMN, flavin mononucleotide; FAD, flavin adenine dinucleotide; ADP, adenosine-5'-diphosphate; PMS, *N*-methylphenazinium methosulfate; PES, phenazine ethosulfate; Os, osmium; PVI-dpaOs, poly-1-vinylimdazole complexed with [osmium(2,2'-dipyridylamine)$_2$Cl]; PEGDGE, poly(ethylene glycol) diglycidyl ether; TAIL-PCR, thermal asymmetric interlaced PCR; PAGE, polyacrylamide gel electrophoresis; EPR, electron spin paramagnetic resonance spectroscopy; ESMS, Electrospray ionization mass spectroscopy; MCES, mediator-assisted continuous-flow column electrolytic spectroelectrochemistry; SHE, standard hydrogen electrode.

INTRODUCTION

The amine oxidoreductases, which are involved in oxidation of amines, are widely distributed to animals, plants, and microorganisms. The well-known class of enzyme is monoamine oxidase (MAO, EC 1.1.3.4) family containing covalently bound FAD (8α-cysteinyl FAD, Figure 1). The reason for this familiarity is the fact that this flavoprotein oxidizes amine hormones and neurotransmitters, compounds regulating behavior of mammalian organisms. Another class of mammalian amine oxidases: histaminase, diamine oxidase, and semicarbazide-sensitive amine oxidase (EC 1.4.3.6) family, was less known so far. During the last two decades, however, this family came to the front, because it was established that they have amino acid modified quinone cofactor, topaquinone (TPQ, Figure 1). A quinone like TPQ appears to be well suited as participant in the conversion of an amine by an oxidase since protein-lysine 6-oxidase (EC 1.4.3.13), oxidizing the lysyl residues in collagen so that cross-links can be formed, has the related lysyl tyrosylquinone (LTQ, Figure 1) as cofactor.

Amines occur as such in nature and they are formed in the pathway of amino acid degaradation via decarboxylation or in that of degradation of substituted amines, e.g. the degradation of choline, or the osmoprotectant betaine and trimethylamine-*N*-oxido, yielding trimethylamine and methylamine. In contrast to mammalian organisms, microbes can utilize these amines as sole carbon and energy source, as sole nitrogen source, or as all. So, a large diversity of amineoxidoreductase appears to be involved in bacterial amine degradation. Several amine dehydrogenases, in particular, have been discovered, and are likely to be key enzymes of respiratory chain in amine degradating bacteria.

Amine dehydrogenases can be widely grouped into quinoprotein family and flavoprotein family; the former is primary amine dehydrogenase family and includes methylamine dehydrogenase (MADH, EC 1.4.99.3) and aromatic amine dehydrogenase (EC 1.4.99.4). These enzymes catalyze the following reaction:

$$RCH_2NH_2 + H_2O + A \rightarrow RCHO + NH_3 + AH_2$$

These enzymes also possess $\alpha_2\beta_2$ subunit structure and one covalently bound tryptophan

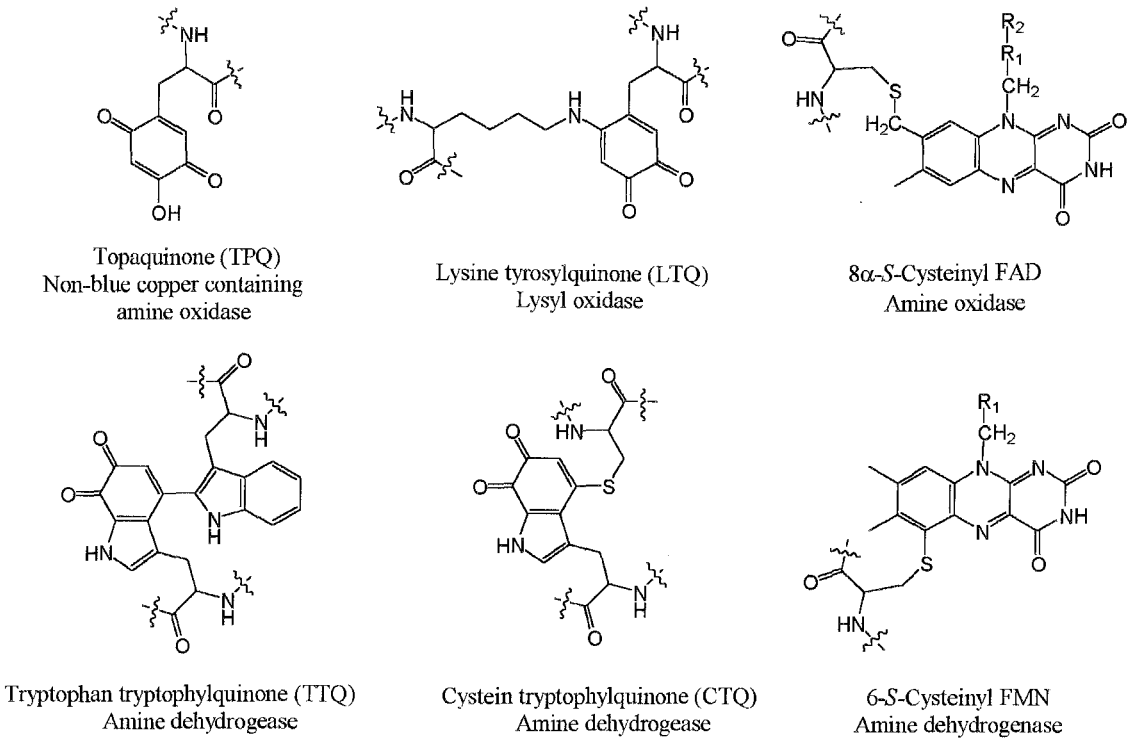

FIGURE 1: Covalently bound flavin derivatives and amino acid modified quinone cofactors. R_1, phosphoribityl; R_2, adenosine-5'-monophosphate.

tryptophylquinone (TTQ, Figure 1) as a prosthetic group in each β subunit. The latter includes trimethylamine dehydrogenase (TMADH, EC 1.5.8.2) and dimethylamine dehydrogenase (DMADH, EC 1.5.8.1). These enzymes catalyze oxidative *N*-demethylation of tertiary and secondary amines:

$$RN(CH_3)_2 + H_2O + A \rightarrow RNH(CH_3) + HCHO + AH_2 \qquad (R = CH_3 \text{ or } H)$$

These enzymes also have a homodimeric structure; each subunit bears a 4Fe-4S cluster and an unusual covalently bound flavin mononucleotide (FMN), 6-*S*-cysteinyl-FMN (Figure 1). These amine dehydrogenases strongly draw our attention due to the rarity of its cofactors, and are also likely to be simple and good examples in biological electron transfer, intra-protein and inter-protein electron transfer, and C-H bond clevage catalyst.

Recently, two novel amine dehydrogenases, quinohemoprotein amine dehydrogenase (QH-AmDH) from *Paracoccus denitrificans* and histamine dehydrogenase (HmDH) from *Nocardioides simplex*, have been discovered. These enzymes catalyze oxidative deamination of primary amines to the corresponding aldehyde and ammonia. QH-AmDH consists of a

heterotrimer and bears two hemes *c* in the largest subunit and one covalently bound cysteine tryptophylquinone (CTQ, Figure 1) in the smallest subunit as a cofactor. HmDH has unique and narrow substrate specificity. So, this enzyme is well suited for application to histamine sensor, but its many characters, such as cofactors and sutructural properties, remain unknown. In this study, these amine dehydrogenases, QH-AmDH and HmDH, are characterized electrochemically and biochemically.

In chapter 1, the author attempted to evaluate the $E^{\circ\prime}$ of the two hemes *c* of QH-AmDH by using MCES through a thermodynamic and kinetic analysis. The γ subunit was isolated and the $E^{\circ\prime}$ value of CTQ and its pH dependence were determined. The author also attempted to measure electron-transfer rate constant between QH-AmDH and two metalloprotein. These data are used to discuss intra- and inter-molecular electron transfer of QH-AmDH from thermodynamic, kinetic, and structural views. The author also characterized a unique inactive hemoprotein, which is very similar to QH-AmDH in structure.

In chapter 2, the author has clarified the primary structure of HmDH from *N. simplex* by PCR methods. The amino acid sequence is highly correlated with that of TMADH and DMADH. This result suggests the presence of 6-*S*-cysteinyl-FMN and 4Fe-4S cluster as the redox centers in HmDH, and the expectation was verified by chemical and spectroscopic analyses. Moreover, sequence alignment study of the three 6-*S*-cysteinyl-FMN-containg enzymes and molecular modeling study based on the crystal coordinates of TMADH were performed for better understanding of the catalytic center, particularly the substrate binding site cavity. The *hmd* gene of HmDH was overexpressed in *Escherichia coli* successfully, and the resulting enzyme was purified to homogeneity. The purified recombinant enzyme is compared with the native enzyme. The author also investigated the possibility to amperometrically detects of histamine using HmDH and osmium-derivative polymer.

CHAPTER 1

Quinohemoprotein Amine Dehydrogenase from *Paracoccus denitrificans*

1. 1. Spectroelectrochemical Evaluation of Redox Potentials of Cysteine Tryptophylquinone and Two Hemes c in Quinohemoprotein Amine Dehydrogenase from Paracoccus denitrificans

Quinoprotein amine dehydrogenases are induced when several methylotrophic bacteria are grown on media including biological amines as the sole source of carbon, nitrogen, and energy (*1*). *Paracoccus denitrificans* NBRC 12442 produces two types of amine dehydrogenases, methylamine dehydrogenase (MADH) (*2*) and quinohemoprotein amine dehydrogenase (QH-AmDH) (*3*), when grown on methylamine and longer chain amines such as *n*-butylamine, respectively. Both enzymes catalyze the oxidation of the primary amines to yield the corresponding aldehyde and ammonia. Aromatic amine dehydrogenase (*4*, *5*) and quinohemoprotein amine dehydrogenase (*6*, *7*), which are structurally very close to MADH and QH-AmDH from *P. denitrificans*, respectively, are expressed in *Alcaligenes faecalis* and *Pseudomonas putida*, respectively.

MADH has an $\alpha_2\beta_2$ quaternary structure, and contains a covalently bound posttranslationally generated quinone cofactor, tryptophan tryptophylquinone (TTQ), on each of the smaller β subunits as the catalytic center, while the larger α subunit does not possess any prosthetic group (*8*). The physiological electron acceptor of MADH is amicyanin, a typical type I copper protein (*9*). Amicyanin is induced together with MADH because the genes encoding these proteins are built in one operon, the *mau* gene cluster (*10*). The electron transfer kinetics from the MADH to amicyanin has been documented (*11*). The redox potential, $E°'$, has been reported as 0.100 V (*12*) or 0.130 V (*13*) for MADH from *P. denitrificans*, and 0.093 V for MADH from bacterium W_3A_1 (*14*). The crystallographic structure of the MADH/amicyanin complex has been determined and shows that hydrophobic residues play an important role in the interaction (*15*). Kinetic and thermodynamic studies coupled with

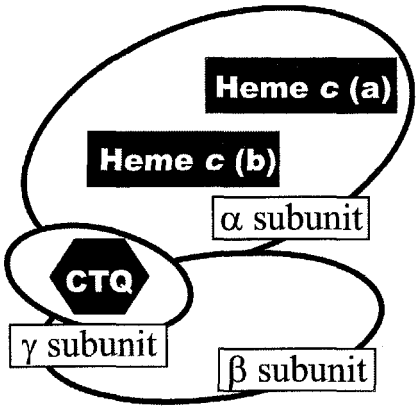

FIGURE 1: Schematic picture of the subunit structure of QH-AmDH.

site-directed mutagenesis have revealed the importance of ionic interactions as well as hydrophobic interactions (*16–18*).

On the other hand, the crystallographic structure of QH-AmDH from *P. denitrificans* and *P. putida* has been recently revealed by two groups, respectively (*19*, *20*). QH-AmDH is a αβγ heterotrimeric protein (Figure 1). The smallest γ subunit has a novel quinone cofactor, cysteine tryptophylquinone (CTQ) (Figure 2), which is formed by posttranslational modification of residues Cys37γ and Trp43γ. The largest α subunit has two heme *c* groups. One of hemes *c* (called heme *c* (a)) is solvent accessible and has His and Met as the first and second axial ligands, respectively, as in the case of the usual cytochrome *c* (*21*). The other one (called heme *c* (b)) is buried almost fully and located between CTQ and heme *c* (a). Heme *c* (b) has *bis*-axial His ligands, as in the case of cytochrome c_3 (*22*). In this respect the diheme-containing domain in the α subunit is similar to diheme cytochrome *c* peroxidase (*23*).

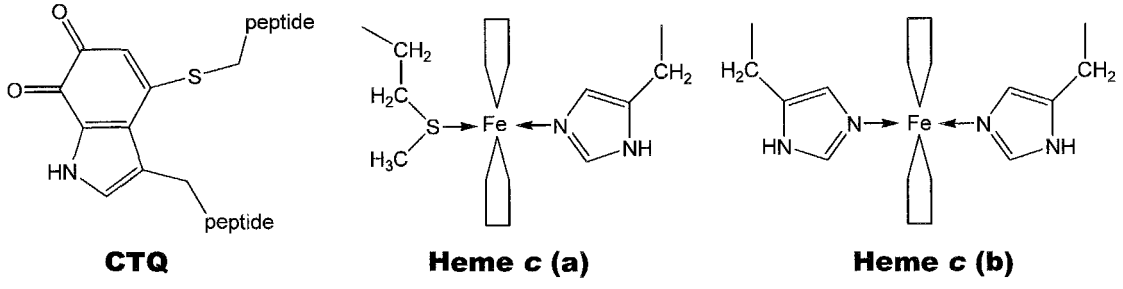

FIGURE 2: Structure of CTQ and schematic features of the axial ligands of the two hemes *c* in QH-AmDH.

Another novel feature of QH-AmDH is that all cysteine residues in the γ subunit are in thioether linkage to Asp or Gln (*19*, *20*). The electron acceptor of QH-AmDH has been found to be cytochrome c_{550} in *P. dentrificans* (*24*) but azurin in *P. putida* (*7*).

For further understandings of the intramolecular electron transfer of QH-AmDH, it is very important to determine $E^{\circ\prime}$ values of all three redox centers in the enzyme (*25*). In a previous paper, our group tried to evaluate $E^{\circ\prime}$ of the heme and quinone groups of QH-AmDH from *P. denitrificans* (*3*) by using a mediator-assisted continuous-flow column electrolytic spectroelectrochemical method (MCES), which has been developed by our groups for protein $E^{\circ\prime}$ measurements (*13*, *26*). The spectroelectrochemical titration curve showed only one step in the redox reaction of the heme group(s) with isosbestic points, which gave a value for $E^{\circ\prime}$ of the heme group(s). The $E^{\circ\prime}$ value of the quinone moiety was indirectly evaluated from the substrate titration curve of the heme group(s). At that time, however, the number of the heme *c* groups was believed to be unity on the basis of the chemical analysis. Therefore, re-evaluation of $E^{\circ\prime}$ is needed.

To date, there are a limited number of reports of $E^{\circ\prime}$ of quinohemoproteins, namely, ethanol dehydrogenase from *Comamonas testosteroni* containing one PQQ and one heme *c* in the molecule (*27*) and membrane-bound alcohol dehydrogenase from *Acetobacter methanolicus* containing one PQQ and four heme *c* groups in the molecule (*28*). The evaluations of $E^{\circ\prime}$ values were based on a conventional redox titration, but were limited to the heme groups. This may be due to small absorption coefficients of the quinone groups compared with those of the heme groups and to the spectroscopic overlapping of the quinone and the heme groups. Our group also applied a column electrolytic spectroelectrochemical method to the $E^{\circ\prime}$ determination of PQQ- and four heme-containing alcohol dehydrogenase (*29*). However, the evaluated data did not lead to a general consensus, since the resulting $E^{\circ\prime}$ values of the heme groups were not in accord with those evaluated by a conventional titration method (*28*). Furthermore, the $E^{\circ\prime}$ value of PQQ was evaluated from small absorption change around the Soret band. Direct electrochemistry of quinohemoproteins (as well as flavohemoproteins) is also very useful from a bioelectrochemical viewpoint (*30–32*). However, the direct electrochemical signal was ascribed only to heme groups if any, and direct electrochemical information concerning organic cofactors has not been obtained.

In this study, the author attempted to re-evaluate the $E^{\circ\prime}$ of the two hemes *c* of QH-AmDH by using MCES through a thermodynamic and kinetic analysis. Since native QH-AmDH gives no direct electrochemical signal, the γ subunit was isolated and the $E^{\circ\prime}$ value of CTQ and its pH dependence were determined. These data are used to discuss intra- and inter-molecular electron transfer of QH-AmDH.

EXPERIMENTAL PROCEDURES

Purifications and Preparations of QH-AmDH. QH-AmDH from *P. denitrificans* was isolated and purified as described in the literature (*3*, *24*) and the concentration of reduced protein was determined from the absorbance at 552 nm (ε = 37.2 $mM^{-1}cm^{-1}$). The fully oxidized and reduced forms of QH-AmDH were prepared by adding $K_3Fe(CN)_6$ and *n*-butylamine or $Na_2S_2O_4$, respectively.

Purification and Preparations of the γ Subunit of QH-AmDH. The γ subunit of QH-AmDH was isolated as follows. A portion of the fully oxidized QH-AmDH was treated with 8 M urea in 100 mM Tris buffer (pH 8.5). The sample was separated by high performance gel filtration chromatography with a Superdex 200 HR 26/60 column and urea-free 50 mM phosphate buffer containing 150 mM NaCl (pH 7.5). The protein concentration was determined by a weighing method, in which the sample was desalted by dialysis against pure water (five times) and lyophilized, or a Bradford method (*33*).

Spectroscopy. UV-visible absorption spectroscopy was recorded with a Shimadzu UV–2500(PC)S or a Shimadzu UV-1500PC photodiode array spectrophotometer with quartz cells of a light path length of 1 cm at room temperature.

Mediator-Assisted Continuous-Flow Column Electrolytic Spectroelectrochemistry (MCES). This technique is based on the spectroscopic detection of the redox states of proteins equilibrated in a continuous-flow redox buffer regulated by column electrolysis (*26*). Potassium ferricyanide, 2,6-dimethylbenzoquinone, *N*-methylphenazinium methosulfate

(PMS), phenazine ethosulfate (PES), 1,4-naphotoquinone, vitamin K_3 and 2-hydroxy-1,4-napthoquinone ($E^{\circ\prime}$ of these compounds at pH 7.0 being 0.443, 0.169, 0.08, 0.055, 0.036, 0.009 and –0.139 V vs. SHE, respectively (*34*)) were used as mediators. In the present study, a portion of a protein sample (usually 10 μL and on the order of 50 μM) was injected on a mobile phase buffer and mixed with a mixed mediator solution in a two-channel flow injection system. Mobile phase buffers used were 0.1 M succinate (pH 6.0), potassium phosphate (pH 7.5), Tris (pH8.0), D-α-alanine (pH 9.0) or carbonate buffers (pH 10.0) at an ionic strength of 0.3 M with KCl. The mixed mediator solution and the mobile phase buffer were thoroughly degassed with argon gas and flowed in the range of 0.35 to 2.0 mL min^{-1}. Other details of the principle, instruments, and methods are described in the literature (*13*, *26*). All potentials in this paper are referred to the standard hydrogen electrode (SHE), unless otherwise stated.

Electrochemistry. Cyclic voltammetry was performed on an HZ-3000 (Hokuto Denko Co.) using an Ag/AgCl/KCl (sat.) reference electrode and a Pt-disk counter electrode. A bare grassy carbon electrode (i.d. 3.0mm, Bioanalytical Systems) as a working electrode was polished with alumina powder (particle size: 0.05 μm) and sonicated in distilled water for about 15 min. The cell was deaerated by passing argon gas through the electrochemical cell for more than 15 min before experiments.

RESULTS

Redox Potentials of Two Hemes c in QH-AmDH. QH-AmDH exhibited reproducible spectral changes depending on the electrode potential (E) in MCES at a flow rate of 0.35 ml min^{-1} at pH 7.0 (0.1 M potassium phosphate, ionic strength 0.3 M with KCl) in the presence of mixed mediators (Figure 3). The spectral change is characteristic of the redox reaction of heme *c* groups. The absorption spectra obtained at 0.4 and –0.1 V were almost identical with those of the fully oxidized form (prepared by the oxidation with $K_3Fe(CN)_6$) and the fully reduced one (prepared by the reduction with *n*-butylamine or $Na_2S_2O_4$), respectively. During the spectral change, the isosbestic points appeared at 342, 411, 440, 510, 538 and 561 nm. Any direct

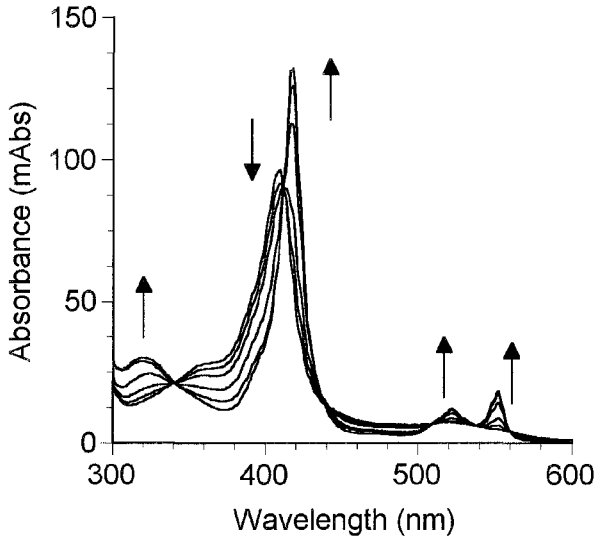

FIGURE 3: Background-corrected absorption spectra of QH-AmDH at 0.397 (fully oxidized), 0.297, 0.222, 0.147, 0.047 and –0.103 V (fully reduced) and at pH 7.0. An aliquot of fully oxidized QH-AmDH sample (50 μM × 10 μL) was injected at each electrode potential to an MCES system with a flow rate of 0.35 ml min^{-1}. Mediators used were 50 μM potassium ferricyanide, 125 μM 2,6-dimethylbenzoquinone, 20 μM *N*-methylphenazinium methosulfate (PMS), 10 μM phenazine ethosulfate (PES), 10 μM vitamin K_3, and 75 μM 2-hydroxy-1,4-napthoquinone. The arrows indicate the direction of the spectral changes on the reduction of QH-AmDH.

information concerning the redox reaction of CTQ was not obtained spectroscopically. The spectra remained practically unchanged in the potential regions of –0.4 to –0.1 V and of 0.4 to 0.6 V.

The *E* dependence of the absorbance at 418 nm (A_{418}) depicted in Figure 4 shows only one-step change. The titration curve was practically independent of the direction and width of the potential step and the flow rate at least up to 0.5 ml min^{-1}. The results strongly support that the redox reaction between QH-AmDH and the mediators reached equilibrium states under the conditions. All these results are practically identical with those reported in a previous paper (*3*).

Since QH-AmDH has two hemes *c* in the molecule, the author hypothesize that the spectral change is assigned to the redox reaction of two hemes *c* alone. Combination of the hypothesis and the one-step sigmoidal characteristics of the titration curve leads to a conclusion that the $E^{\circ\prime}$ value of heme *c* (b) with His as the second axial ligand is close to that

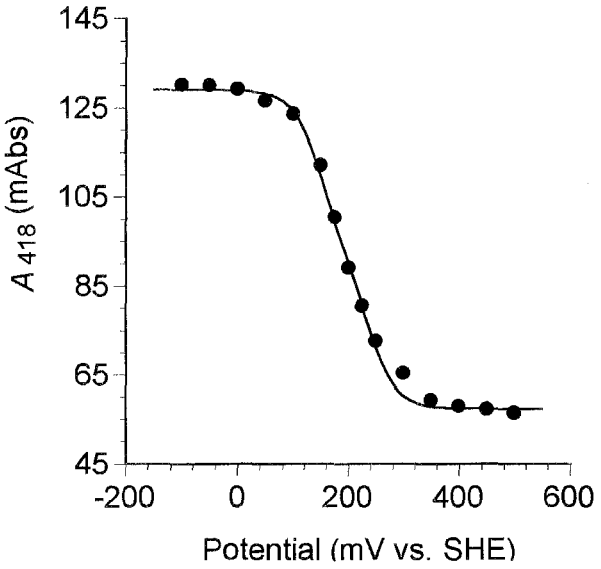

FIGURE 4: Spectroelectrochemical titration curve of QH-AmDH taken by the MCES method under equilibrated conditions, of which the details are given in the caption of Figure 3. (•) Experimental data; (–) nonlinear regression curve calculated based on eq 3.

of heme *c* (a) with Met as the second axial ligand. However, this conclusion appears to contradict the reported characteristics of hemes *c* with *bis*-His axial ligands, which have fairly negative $E^{\circ\prime}$ values compared with usual hemes *c* with Met as the second axial ligand (*35*). In addition, combination of the hypothesis and the appearance of the isosbestic points in the spectral change leads to another conclusion that heme *c* (b) is strongly similar to heme *c* (a) in the spectral property in spite of the difference in the second axial ligand. Therefore, it is very important and indispensable to confirm the hypothetical assignment of the spectral change in the one-step sigmoidal titration curve.

Kinetic Distinction between Heme c (a) and Heme c (b). For the above purpose, the author attempted to distinguish heme *c* (b) from heme *c* (a) by a kinetic analysis. The MCES method is useful to obtain kinetic information on the electron transfer between proteins and mediators, where the reaction time is controlled by the flow rate (*13*). At increased flow rates, the spectrum of QH-AmDH electrolyzed on the MCES system depended on the flow rate. This means that QH-AmDH was eluted before reaching equilibrium with the mediators. Under such kinetically controlled conditions, the A_{418} vs. E curve clearly showed two-step

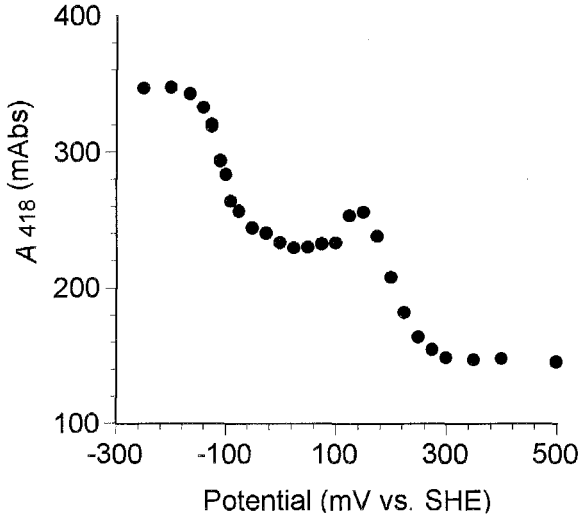

FIGURE 5: Absorbance at 418 nm (A_{418}) of QH-AmDH as a function of the electrode potential (E) taken by the MCES method under non-equilibrium high flow rate conditions at pH 7.0. 10 μL of the fully oxidized species 50 μM was injected at each E. The flow rate of MCES was 2 ml min^{-1}, and the mediators used are 50 μM potassium ferricyanide, 125 μM 2,6-dimethylbenzoquinone, 10 μM vitamin K_3, and 75 μM 2-hydroxy-1,4-napthoquinone.

characteristics, as shown in Figure 5, where the flow rate was 2.0 ml min^{-1}, and PMS and PES were removed from the mixed mediator solution to reduce the rate of the electron exchange between QH-AmDH and the mediators. The appearance of the two-step wave reflects the difference in the reduction kinetics of the two hemes *c* (Note that the oxidized form of QH-AmDH was injected for each data point in this case). The absorbance of QH-AmDH in Figure 5 was larger than that in Figure 4 in spite of the same amount of injected protein, which is due to the cause that dilution and diffusion of protein sample in the column are relatively suppressed at increased flow rates, leading to sharp elution peaks. Other spectral properties were almost identical with those obtained under equilibrium conditions, although the titration curve showed a peak shape in the first step of reduction. The observation of the two-step redox curves strongly supports the hypothetical assignment that the one-step characteristics of the titration curve under equilibrated conditions reflect the sequential redox reaction of the two hemes *c* groups.

Evaluation of E^{o}' of Two Heme c Groups. The Nernst equations of the heme groups (H_L

and H_H, L and H denoting the hemes with lower and higher $E^{\circ\prime}$, respectively) are given by:

$$\frac{[H_{L,ox}]}{[H_{L,red}]} = \exp\left[\frac{F}{RT}(E - E^{\circ\prime}_L)\right] \equiv \eta_L \quad (1)$$

$$\frac{[H_{H,ox}]}{[H_{H,red}]} = \exp\left[\frac{F}{RT}(E - E^{\circ\prime}_H)\right] \equiv \eta_H \quad (2)$$

where the subscripts ox and red denote the oxidized and reduced forms of the heme, respectively. The square brackets mean the concentration of the corresponding species, and F, R, and T have the usual meaning. Here, the author assumes that two heme c groups undergo the redox reaction independently. Since CTQ-related absorption coefficient would be negligibly small as compared with that of two hemes c, the relationship between the absorbance (A) and E can be expressed by

$$\begin{aligned} A &= (\varepsilon_{L,ox}[H_{Lox}] + \varepsilon_{L,red}[H_{L,red}] + \varepsilon_{H,ox}[H_{H,ox}] + \varepsilon_{H,red}[H_{H,red}])l \\ &= \frac{\eta_H A_1}{\eta_H + 1} + \frac{(\eta_L - \eta_H)A_2}{(\eta_H + 1)(\eta_L + 1)} + \frac{A_3}{\eta_L + 1} \end{aligned} \quad (3)$$

with

$$A_1 = (\varepsilon_{H,ox} + \varepsilon_{L,ox})[P]l \quad (4)$$

$$A_2 = (\varepsilon_{H,red} + \varepsilon_{L,ox})[P]l \quad (5)$$

$$A_3 = (\varepsilon_{H,red} + \varepsilon_{L,red})[P]l \quad (6)$$

where $\varepsilon_{L,ox}$, $\varepsilon_{L,red}$, $\varepsilon_{H,ox}$, and $\varepsilon_{H,red}$ are the absorption coefficients of the corresponding species, [P] (= $[H_{L,ox}] + [H_{L,red}] = [H_{H,ox}] + [H_{H,red}]$) denotes the total concentration of QH-AmDH, and l is the light-path length ([P]l being constant under the experimental conditions). The A value reduces to A_1 at $E >> E^{\circ\prime}_H > E^{\circ\prime}_L$ ($\eta_H > \eta_L >> 1$), or to A_3 at $E << E^{\circ\prime}_L < E^{\circ\prime}_H$ ($\eta_L < \eta_H << 1$), and then A_1 and A_3 can be evaluated experimentally from the plateaus of the titration curve in Figure 4. Considering the close similarity of the spectroscopic property of the two hemes, it can be reasonably assumed that $\varepsilon_{L,ox} \approx \varepsilon_{H,ox}$ and $\varepsilon_{L,red} \approx \varepsilon_{H,red}$; that is, $A_2 \approx (A_1 + A_3)/2$. Therefore, eq 3 can be fitted to the titration curve using $E^{\circ\prime}_H$ and $E^{\circ\prime}_L$ (or η_H and η_L) as the adjustable parameters by nonlinear regression analysis. The Nernstian analysis yielded 0.235 ± 0.006 V and 0.149 ± 0.003 V for $E^{\circ\prime}_H$ and $E^{\circ\prime}_L$, respectively (the deviation being given as the goodness of the fitting). The regression curve can well reproduce the experimental data, as shown by the solid line in Figure 4.

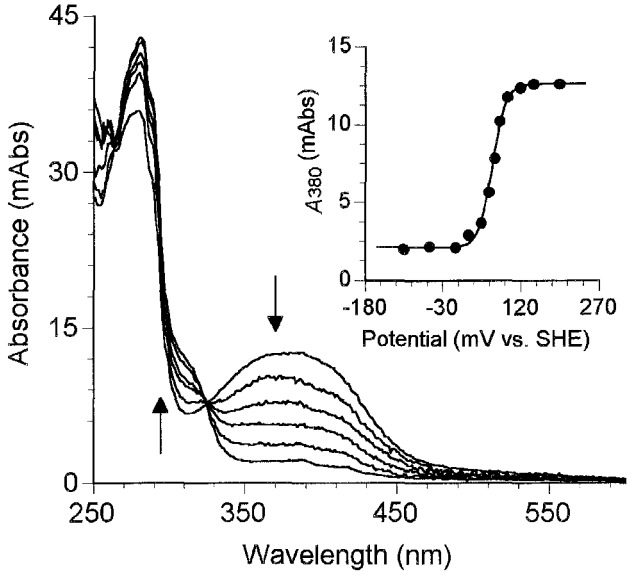

FIGURE 6: Background-corrected absorption spectra of the γ subunit of QH-AmDH at 0.193 (fully oxidized), 0.078, 0.068, 0.058, 0.043, and –0.057 V (fully reduced) at pH 7.0. An aliquot of the γ subunit (50 μM × 10 μL) was injected to an MCES system with a flow rate of 0.35 ml min^{-1} at each electrode potential. Mediators used were 30 μM *N*-methylphenazinium methosulfate (PMS) and 20μM phenazine ethosulfate (PES). The arrows indicate the direction of the spectral changes on the reduction of the γ subunit. Inset: Spectroelectrochemical titration curve of the γ subunit obtained by the MCES method at 380 nm. (•) Experimental data; (–) nonlinear regression curve on the basis of a one-step two-electron transfer model.

Purification and Spectral Properties of the γ Subunit. The gel chromatographic separation of urea-treated QH-AmDH yielded three major peaks. The molecular mass of the third peak was assessed to be ca. 9 kDa, which is close to the calculated one of the γ subunit (8.5 kDa) (*19*). Then, it can be concluded that the third peak corresponds to the γ subunit of QH-AmDH. When the γ subunit fraction was re-assayed by gel chromatography, the retention time was almost identical with that of the first one. Therefore, it can be concluded that the isolated γ subunit is monomeric even in the absence of urea. The γ subunit oxidized with $K_3Fe(CN)_6$ gave a characteristic broad absorption band centered at 380 nm. This absorption band overlaps with the Soret band of QH-AmDH. The absorption coefficients were evaluated as 7 mM^{-1} cm^{-1} at 380 nm when the peptide contents were evaluated by the weighing method, while a value of 14 mM^{-1} cm^{-1} was obtained from the peptide content data by the Bradford

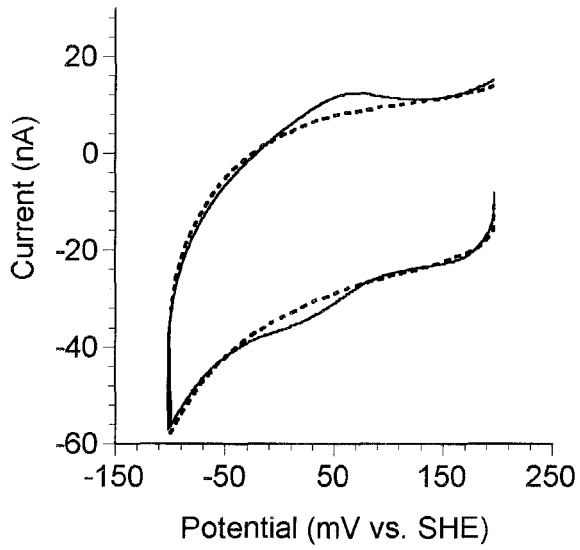

FIGURE 7: Cyclic voltammograms of the γ subunit of QH-AmDH. Solid and broken lines are cyclic voltammogram in the presence and absence of 5.2 μM of the γ subunit, respectively, at a glassy carbon electrode at a scan rate of 5 mV s^{-1} in 0.05 M potassium phosphate (pH 7.0).

method. The value(s) is significantly smaller than that of the Soret band of QH-AmDH (227 mM^{-1} cm^{-1} at 408 nm for the fully oxidized species (*3*)). Addition of substoichiometric amounts of $Na_2S_2O_4$ to the γ subunit caused a decrease in the broad band around 380 nm. However, it was difficult to obtain the absorption of spectrum of the fully reduced form due to spectral overlap with $Na_2S_2O_4$. The γ subunit retained dehydrogenase activity for *n*-butylamine with $K_3Fe(CN)_6$ as an electron acceptor, but the activity is very low (10^4 times lower than the native QH-AmDH). The γ subunit was slightly unstable at room temperature, the lifetime being about 5 h, as judged from spectral change.

Electrochemistry of the γ Subunit. The MCES method has the capacity to obtain background-corrected absorption spectra of proteins in the presence of mediators (*13*, *26*). In order to determine the absorption spectrum of the fully reduced form, the isolated γ subunit was analyzed by the MCES method at a flow rate of 0.35 ml min^{-1} at pH 7.0 in the presence of mixed mediators. The column electrode reduction of the γ subunit caused a decrease in the broad band around 380 nm and an increase in a new shoulder band around 315 nm, giving an

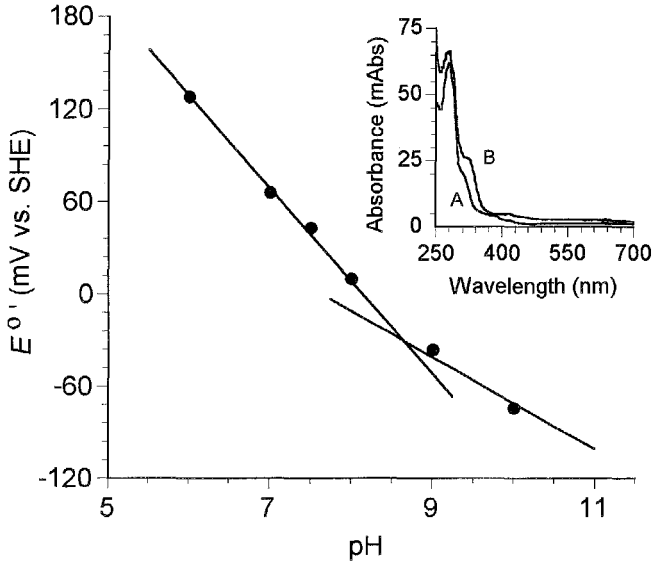

FIGURE 8: $E°'$ of CTQ in the isolated γ subunit as a function of pH. The slopes of the two straight lines are –60 and –30 mV/pH. Mediators used were identical with those given in Figure 6, except at pH 10.0 where 15 μM PMS and 150 μM 1,4-naphotoquinone were used. Inset: The absorption spectra of the fully reduced form of the isolated γ subunit with (3.3 μM) at pH 6.0 (A) and 10.0 (B). The spectra were obtained by the MCES method.

isosbestic point at 326 nm, as shown in Figure 6. The spectroelectrochemical titration curve showed a nernstian response (Figure 6, inset), and was well reproduced on the basis of a one-step two-electron transfer model (*13*, *36*, *37*). The nonlinear regression analysis of the titration curve yielded $E°'$ of 0.065 ± 0.002 V at pH 7.0.

The isolated γ subunit gave a pair of cathodic and anodic waves on a cyclic voltammogram at a bare glassy carbon electrode (Figure 7). This redox wave is reasonably assigned to CTQ. The peak separation was ca. 50 mV at a scan rate (v) of 5 mV s^{-1}. However, the peak currents were proportional to v, and almost independent of the concentration (at least at 2 μM and larger), indicating quasi-reversible characteristics due to the adsorbed species of the γ subunit. The midpoint potential was evaluated to be 0.042 V at pH 7.0.

Figure 8 shows the pH dependence of $E°'$ of the CTQ cofactor in the isolated γ subunit, $E°'$ being evaluated by the MCES method. Changes of –60/pH and –30/pH units were observed with an inflection at pH 8.6. The results indicate that the two-electron transfer of CTQ is linked to the transfer of two protons at pH < 8.6, and of single proton at pH > 8.6. The

pH value of the inflection point (8.6) corresponds to pK_a value of the quinol form of CTQ (*38*), K_a being the acid dissociation constant. A red shift of the shoulder band (longest π–π^* band) of the quinol form was observed upon the deprotonation of the quinol form, as shown in the inset of Figure 8, while the absorption spectrum of the oxidized CTQ remained unchanged in the pH region examined (pH 6–10) (data not shown).

DISCUSSION

This study has, for the first time, revealed the absorption spectra of the fully oxidized and reduced CTQ bound to the γ subunit of QH-AmDH. The fully oxidized form gave a characteristic broad absorption band around 380 nm with an absorption coefficient of 7 mM^{-1} cm^{-1} by the weighing method as a peptide content assay (or 14 mM^{-1} cm^{-1} by the Bradford method). The wavelength and the absorption coefficient of the longest π–π^* band of CTQ are, respectively, shorter and smaller than those of TTQ enzymes (about 450 nm and about 20–25 mM^{-1} cm^{-1}, respectively, (*5, 12*). The small increase in the shoulder band of the fully reduced CTQ around 315 nm is also compared with a large increase seen with TTQ enzymes upon the reduction (*5, 12*). These differences in the spectroscopic properties of CTQ from TTQ seem due to decreased π-stabilization of tryptophylquinone and its quinol by cross-linking to Cys instead of aromatic Trp, although the π conjugation in a free state of a TTQ model compound is not so strong (*38*).

The absorption coefficient of CTQ and its change upon the redox reaction is very small compared with those of the Soret band of the heme groups. In addition, the absorption band of CTQ partially overlaps with the Soret band. These are the reasons why it was very difficult to extract the information on the redox reaction of CTQ from the spectral change of QH-AmDH. This consideration also indicates that the spectral change of QH-AmDH reflects the redox reaction of the heme *c* groups alone.

The isolated γ subunit gave a direct electrochemical signal of CTQ at a bare glassy carbon electrode. This is very interesting, since direct electrochemistry has not yet been achieved for quinone cofactors of quinoproteins. Most probably, the small size of the γ subunit is responsible for the successful observation of the direct electron transfer to/from the

electrode. However, the response was ascribed to the adsorbed species, so that the midpoint potential (0.042 V) evaluated from the voltammogram includes the difference in the adsorption energy between the fully oxidized and reduced γ subunit (*39*, *40*). In contrast, the MCES method provided information concerning the soluble species under equilibrated conditions, and the midpoint potential (0.065 V) evaluated by MCES (Figure 6) is more reliable for $E^{\circ\prime}$ of the CTQ cofactor, in this case, than that of cyclic voltammetry. The latter is slightly more negative than the former, suggesting that the fully reduced γ subunit adsorbs more strongly on the electrode than the fully oxidized one (*39*).

The $E^{\circ\prime}$ value of CTQ evaluated in this work could be somewhat different from that of the native one, because the isolated γ subunit is likely to be less structured than it is in the complete QH-AmDH. However, the $E^{\circ\prime}$ value is close to that of TTQ in MADH from *P. denitrificans* (0.100 V at pH 7.5, (*12*); 0.130 V at pH 7.5, (*13*)) and that of a TTQ model compound (0.107 V at pH 7.0 (*38*)). This result seems to be reasonable since both CTQ and TTQ have the same tryptophylquinone skeleton. Therefore, the $E^{\circ\prime}$ value of CTQ evaluated here can be accepted as that of the native one to a first approximation.

The two- and single-proton transfer linked to the two-electron transfer of CTQ and pK_a (8.6) of one of the phenolic OH groups of the quinol form are compared with TTQ. In MADH, the single-proton transfer is linked to the two-electron transfer in the pH range of 6.2 to 8.3 (*41*), indicating that the pK_a value of the TTQ quinol in MADH is less than 6. In a TTQ model compound, a two-proton transfer occurs at pH < 10 and pK_a of the TTQ quinol is 10.1 (*38*). The difference may be explained by the difference in the environments of the quinone cofactors: the γ subunit could be disordered in part and CTQ is more solvent accessible than TTQ in MADH.

There was no evidence for the presence of the semiquinone form of CTQ in the redox titration or in the spectral change. This result suggests that the one electron redox potential of CTQ and the semiquinone couple is more negative by about 100 mV than that of the semiquinone and the fully reduced CTQ couple for the isolated γ subunit (*40*). In contrast, for QH-AmDH an ESR signal of the semiquinone has been observed upon partial reduction (*3*), indicating thermodynamic stabilization of CTQ semiquinone in the enzyme. Destabilization of semiquinone in the isolated γ subunit would be due to an increased solvent accessibility of

CTQ.

The γ subunit exhibited dehydrogenase activity for *n*-butylamine with $K_3Fe(CN)_6$ as an electron acceptor, although the activity was very low. Such behavior can be expected, since all the other quinone cofactors show similar catalytic activity for oxidative deamination of amines (such as benzylamine) in the free state (*38, 42–45*). However, the author did not carry out further kinetic experiments (for example, on substrate or co-substrate specificity), since the γ subunit could be in part denatured.

This study also has clearly revealed that the one-step profile of the spectroelectrochemical titration curve (Figure 4) can be ascribed to the redox reaction of the two hemes *c* in QH-AmDH. The appearance of the isosbestic points in the titration curve (Figure 3) indicates that the spectral properties of heme *c* (a) and heme *c* (b) are very close to each other in spite of the difference in the second axial ligand. Based on these considerations, the titration curve was successfully analyzed using a model in which two hemes *c* groups undergo the redox reaction independently (independent model) yielding $E^{\circ\prime}{}_H$ and $E^{\circ\prime}{}_L$. An alternative model involving an interactive two-step one-electron transfer, where $E^{\circ\prime}$ of one heme depends on the redox state of the other heme (interactive model), also was applied to the analysis of the titration curve. The major difference in the interpretation of titration curves between the two models appears only in the case when the two $E^{\circ\prime}$ become close to each other or are reversed with respect to each other. The cooperative multi-step redox reactions in the interactive model occur in proton transfer-coupled electron transfers (as in the case of quinones) (*13, 37, 40, 46*) or conformational change-coupled electron transfers (*47, 48*). In my case, the result analyzed by the interactive model was identical to that obtained with the independent model (data not shown). Therefore, the author cannot conclude from the thermodynamic analysis whether the two hemes *c* groups interact with each other. However, since the distance between two iron atoms of hemes *c* (a) and (b) is about 16 Å (*19*), the interaction would not be so strong, if at all.

The other interesting feature is that the two hemes *c* were well distinguished from each other with respect to the reduction kinetics of QH-AmDH with the mediators. The A_{418} vs. E profile under non-equilibrium conditions (Figure 5) gave apparent midpoint potentials of the first and second one-electron reductions as about 0.2 and –0.1 V, respectively. The former is

relatively close to the $E^{\circ\prime}_{H}$ value (0.235 V) evaluated by MCES under equilibrated conditions, but the latter is more negative than $E^{\circ\prime}_{L}$ (0.149 V). This suggests that the reduction of the heme *c* of $E^{\circ\prime}_{H}$ with mediators is fast compared with the other heme. Most probably, the heme *c* of $E^{\circ\prime}_{H}$ is more solvent-accessible than the other. Considering the crystallographic structure of QH-AmDH (*19*), the heme *c* of $E^{\circ\prime}_{H}$ is reasonably assigned to heme *c* (a) with Met as the second axial ligand, and the other is assigned to heme *c* (b) with His as the second axial ligand. This assignment is consistent with the nature of the iron ligation (*35*).

One question arises here on the A_{418} vs. E profile under the kinetic conditions: why does the first one-electron reduction step show a peak shape (Figure 5)? The reason is not clear, but the electrode potential where the peak shape appeared (ca. 0.14 V) is close to $E^{\circ\prime}$ of 2,6-dimethylbenzoquinone (0.169 V), one of the mediators used. This mediator is susceptible to adsorption on the carbon fiber electrode surface in the column electrode, and the adsorption coefficients of the oxidized and reduced form must be different. In addition, the electron transfer rate from the mediator to QH-AmDH would be affected by the soluble or adsorbed states of mediators. This might be one of the causes of the appearance of the peak in the titration curve. Note that such an adsorption effect (or kinetic effect) does not disturb the titration curve under equilibrated conditions.

The $E^{\circ\prime}$ value of heme *c* (a) is close to that of horse heart cytochrome *c* (0.255 V (49)) and cytochrome c_{550} (0.243 V (24)), both of which having Met as the second axial ligand. On the other hand, *bis*-His axial hemes *c* occurs in cytochrome c_3 from *Desulfovibrio vulgaris* (*22*) and in tetra-heme *c*-type cytochrome from *Paracoccus denitrificans* (*50*). The $E^{\circ\prime}$ values of these hemes *c*, which locate in the range of –0.4 to 0 V, are more negative than those of usual cytochromes *c* (*34, 35, 50–52*). It has also been reported that the second axial ligand replacement of His with Met in one of the four hemes *c* in cytochrome c_3 causes a large positive shift in $E^{\circ\prime}$ by at least 0.2 V (*53*). Further, the $E^{\circ\prime}$ values of two hemes *c* in diheme cytochrome *c* peroxidase have been reported as 0.320 V and –0.330 V, of which the second axial ligand are Met and His, respectively (*23*). Heme *c* (b) of QH-AmDH is only 0.086 V more negative in $E^{\circ\prime}$ than heme *c* (a), and considerably more positive than the *bis*-His axial hemes *c* reported so far. This is a very interesting feature, and such an unusual thermodynamic property might be due to the low solvent-accessibility of the heme *c* (b) in QH-AmDH.

The crystal structure of QH-AmDH (*19*) suggests that the electron transfer pathway from CTQ to heme *c* (a) occurs via heme *c* (b) (Figure 1). The present thermodynamic study supports this prediction. The $E^{\circ\prime}$ values of these redox centers are located in this case from the negative to the positive direction.

Cytochrome c_{550}, the physiological electron acceptor of QH-AmDH in *P. denitrificans*, has $E^{\circ\prime}$ of 0.243 V (pH 7.5) (*24*), which is slightly more positive than that of heme *c* (a). Heme *c* (a) is more solvent accessible and is located in more hydrophilic environment than heme *c* (b) (*19*). These properties of heme *c* (a) seem to be reasonable for it to function as an electron-donating site to the hydrophilic cytochrome c_{550}. However, it is very important to note that very fast electron transfer ($k_{cat} = 4.7\ s^{-1}$, $K_M \leq 0.1\ \mu M$, $k_{cat}/K_M \geq 4.7 \times 10^7\ M^{-1}s^{-1}$) occurs from heme *c* (a) to cytochrome c_{550} despite the relatively small difference in $E^{\circ\prime}$(*54*). This may be due to the short distance in the two redox centers and low reorganization (*55*). The proposed inter-protein electron transfer in QH-AmDH is compared with that of MADH/amicyanin, where hydrophobic interactions play an important role (*15*) and the difference in $E^{\circ\prime}$ is as large as 0.1 V, although ionic interactions also function cooperatively (*16–18*). For more detailed understanding of these intra- and inter-protein electron transfer reactions, structural analysis of QH-AmDH/cytochrome c_{550} complex and kinetic and thermodynamic analyses coupled with site-directed mutagenesis will be required.

SUMMARY

Quinohemoprotein amine dehydrogenase (QH-AmDH) from *Paracoccus denitrificans* has a novel cofactor cysteine tryptophylquinone (CTQ) in the smallest γ subunit and two hemes *c* in the largest α subunit (Datta, S., Mori, Y., Takagi, K., Kawaguchi, K., Chen, Z., Okajima, T., Kuroda, S., Ikeda, T., Kano, K., Tanizawa, K., and Mathews, F. S. (2001) *Proc. Natl. Acad. Sci. USA, 98*, 14268–14273.). The spectral change of QH-AmDH was assigned to the redox reaction of the hemes *c* alone. The redox potentials of the two hemes *c* with His and Met as the second axial ligands, respectively, were determined to be 0.149 V and 0.235 V vs. SHE at pH 7.0 by a mediator-assisted continuous-flow column electrolytic spectroelectrochemical technique (MCES). The monomeric γ subunit of QH-AmDH was

isolated from urea-treated QH-AmDH. The fully oxidized and reduced forms of the γ subunit exhibited a unique absorption band centered at 380 nm and a shoulder band around 315 nm, respectively, at neutral pH. The two-electron redox potential of CTQ in the isolated γ subunit was evaluated to be 65 mV at pH 7.0 by MCES. The redox reaction was linked to the two-proton transfer at pH < 8.6 and to a single-proton transfer at pH > 8.6, The pK_a value (K_a: acid-dissociation constant) of 8.6 was assigned to one of the phenolic OH groups of the quinol form. Upon the deprotonation, the red shift of the shoulder band was observed. The γ subunit adsorbed on a glassy carbon electrode, and gave a direct but quasi-reversible electrochemical signal. Intra- and inter-protein electron transfers of QH-AmDH are discussed from thermodynamic and structural viewpoints.

REFERENCES

1. Anthony, C. (1990) *Antonie van Leeuwenhoek 56*, 13–23.
2. Husain, M. and Davidson, V. L. (1987) *J. Bacteriol. 169*, 1712–1717.
3. Takagi, K., Torimura, M., Kawaguchi, K., Kano, K., and Ikeda, T. (1999) *Biochemistry 38*, 6935–6942.
4. Iwaki, M., Yagi, T., Horiike, K., Saeki, Y., Ushijima, T., and Nozaki, M. (1983) *Arch. Biochem. Biophys. 220*, 253–262.
5. Govindaraj, S., Eisenstein, E., Jones, L. H., Sanders-Leohr, J., Chistoserdov, A. Y., Davidson, V. L., and Edwards, S. L. (1994) *J. Bacteriol. 176*, 2922–2929.
6. Shinagawa, E., Matsushita, K., Nakashima, K., Adachi, O., and Ameyama, M. (1998) *Agric. Biol. Chem. 52*, 2255–2263.
7. Adachi, O., Kubota, T., Hacisalihoglu, A., Toyama, H., Shinagawa, E., Duine, J. A., and Matsushita, K. (1998) *Biosci. Biotechnol. Biochem. 62*, 469–478.
8. McIntire, W. S., Wemmer, D. E., Chistoserdov, A. and Lidstrom, M. E. (1991) *Science 252*, 817–824.
9. Husain, M. and Davidson, V. L. (1985) *J. Biol. Chem. 260*, 14626–14629.
10. Chistoserdov, A., Y., Boyd, J., Mathews, F. S., and Lidstrom, M., E. (1992) *Biochem. Biophys. Res. Commun. 184*, 1181–1189.

11. Davidson, V., L. and Jones, L. H. (1991) *Anal. Chim. Acta 249*, 235–240.

12. Husain, M. and Davidson, V. L. (1987) *Biochemistry 26*, 4139–4143.

13. Sato, A., Torimura, M., Takagi, K., Kano, K., and Ikeda, T. (2000) *Anal. Chem. 72*, 150–155.

14. Burrows, A., L., Hill, H., A., Leese, T., A., Mcintire, W., S., Nakayama, H., and Sanghera, G., S. (1991) *Eur. J. Biochem. 199*, 73–78.

15. Chen, L., Durley, R., Poliks, J. B., Hamada, K., Chen, Z., Mathews, F., S., Davidson, V. L., Satow, Y., Huizinga, E. Vellieux, F. M. D., and Hol, W. G. J. (1992) *Biochemistry 31*, 4959–4964.

16. Davidson V. L., Johns, L. H., Graichen, M. E., Mathews, F. S., Hosler, J. P. (1997) *Biochemistry, 36*, 12733–12738.

17. Zhu, Z., Curane, L. M., Chen, Z., Durley, R. C. E., Mathews, F. S., and Davidson, V. L. (1998) *Biochemistry 37*, 17128–17136.

18. Zhu, Z., Johns, L. H., Graichen, M. E., Davidson, V. L. (2000) *Biochemistry 39*, 8830–8836.

19. Datta, S., Mori, Y., Takagi, K., Kawaguchi, K., Chen, Z., Okajima, T., Kuroda, S., Ikeda, T., Kano, K., Tanizawa, K., and Mathews, F. S. (2001) *Proc. Natl. Acad. Sci. U.S.A. 98*, 14268–14273.

20. Satoh, A., Kim, J., K., Miyahara, I., Devreese, B., Vandenberghe, I., Hacisalihoglu, A., Okajima, T., Kuroda, S., Adachi, O., Duine, J., A., Van Beeumen, J., Tanizawa, K., and Hirotsu, K. (2002) *J. Biol. Chem. 277*, 2830–2834.

21. Timkovich, R. and Dickerson, R., E. (1975) *J. Biol. Chem. 251*, 4033–4046.

22. Higuchi, Y., Bando, S. Kusunoki, M., Matsuura, Y., Yasuoka, N., Kakudo, M., Yamanaka, T., Yagi, T. and Inokuchi, H. (1981) *J. Biochem. 89*, 1659–1662.

23. Fülöp, V., Ridout, C., J., Greenwood, C., and Hajdu, J. (1995) *Structure* 3, 1225–1233.

24. Takagi, K., Yamamoto, K., Kano, K., and Ikeda, T. (2001) *Eur. J. Biochem. 268*, 470–476.

25. Klinman, J. P. (2001) *Proc. Natl. Acad. Sci. U.S.A. 98*, 14766–14768.

26. Torimura, M., Mochizuki, M., Kano, K., Ikeda, T., and Ueda, T. (1998) *Anal. Chem. 70*, 4690–4695.

27. Dejong, G., A., H., Caldeira, J., Sun, J., Jongejan, J., A., Devries, S., Loehr, T., M., Moura,

I., Moura, J., J., G., Duine, J., A. (1995) *Biochemistry 34*, 9451–9458.

28. Frébortova, J., Matsushita, K., Arata, H. and Adachi, O. (1998) *Biochim. Biophys. Acta 1363*, 24–34.
29. Torimura, M., Kano, K., Ikeda, T., and Ueda, T. (1997) *Chem. Lett. 6*, 525–526.
30. Ikeda, T., (1997) in *Frontiers in Biosensorics I, Fundamental Aspects*, (Scheller, F. W. and Schubert, F., and Fedrowitz, J., Eds.) pp. 243–266, Birkhäuser Verlag Basel, Switzerland.
31. Ikeda, T., Miyaoka, S., and Miki, K. (1993) *J. Electroanal. Chem. 352*, 267–278.
32. Lindgren, A., Larsson, T., Ruzgas, T., and Gorton, L. (2000) *J. Electroanal. Chem. 49*, 105–113.
33. Bradford, M. M. (1976) *Anal. Biochem. 72*, 248–254.
34. Kano, K. (2002) *Rev. Polarogr. 48*, 29–46.
35. Mathews, F., S., (1985) *Prog. Biophys. Mol. Biol. 45*, 1–56.
36. Torimura, M., Mochizuki, M., Kenji, K., Ikeda, T., and Ueda, T. (1998) *J. Electroanal. Chem. 451*, 229–235.
37. Sato, A., Takagi, K., Kano, K., Kato, N., Duine, J.A., Ikeda, T. (2001) *Biochem. J. 357*, 893–898.
38. Itoh, S., Ogino, M., Haranou, S., Terasaka, T., Ando, T., Komatsu, M., Ohshiro, Y., Fukuzumi, S., Kano, K., Takagi, K. and Ikeda, T. (1995) *J. Am. Chem. Soc. 117*, 1485–1493.
39. Bard, A. J. and Faulkner, L. R. (2001) *Electrochemical Methods: Fundamentals and Applications*, 2nd ed., pp.590–593, Wiley, New York.
40. Kano, K., and Uno, B. (1993) *Anal. Chem. 65*, 1088–1093.
41. Zhu, Z. and Davidson, V. L. (1998) *J. Biol. Chem. 273*, 14254–14260.
42. Itoh, S., Takada, N., Haranou, S., Ando, T., Komatsu, M., Ohshiro, Y. and Fukuzumi, S. (1996) *J. Org. Chem. 61*, 8967–8974.
43. Mure, M., Klinman, J., P. (1995) *J. Am. Chem. Soc. 117*, 8698–8706.
44. Kano, K., Nakagawa, M., Takagi, K., Ikeda, T. (1997) *J. Chem. Soc. Perkin Trans. 2*, 1111–1119.
45. Akagawa, M. and Suyama, K., (2001) *Biochem. Biophys. Res. Commun. 281*, 193–199.
46. Wipf, D. O., Wehmeyer, K. R., and Wightman, R. M. (1986) *J. Org. Chem. 51*,

4760–4764.

47. Pierce D. T. and Geiger, W. E. (1989) *J. Am. Chem. Soc. 111*, 7636–7638.
48. Kano, K., Sugimoto, T., Misaki, Y., Enoki, T., Hatakeyama, H., Oka, H., Hosotani, Y., Yoshida, Z. (1994) *J. Phys. Chem. 98*, 252–258.
49. Eddowes, M., J., and Hill, H., A., O. (1979) *J. Am. Chem. Soc. 101*, 4461–4464.
50. Roldán, M. D., Sears, H. J., Cheesman, M. R., Ferguson, S. J., Thomson, A. J., Berks, B. C. and Richardson, D. J. (1998) *J Biol. Chem. 273*, 28785–28790.
51. Moore, G. R., and Pettigrew, G. W. (1990) *Cytochromes c: Evolutionary, Structural and Physicochemical Aspects*, Springer-Verlag, Berlin.
52. Sokol, W., F., Evans, D., H., Niki, K., and Yagi, T. (1980) *J. Electroanal. Chem. 108*, 107–115.
53. Mus-Veteau, I., Dolla, A., Guerlesquin, F., Payan, F., Czjzek, M., Haser, R., Bianco, P., Haladjian, J., Rapp-Giles, B. J. and Wall, J. D. (1992) *J. Biol. Chem. 267*, 16851–16858.
54. Fujieda, N., Mori, M., Kano, K., and Ikeda, T. (2003) *Biochem. Biophys. Acta 1647*, 289–296
55. Davidson, V. L. (2000) *Acc. Chem. Res. 33*, 87–93.

1. 2. Redox Properties of Quinohemoprotein Amine Dehydrogenase from Paracoccus denitrificans

Paracoccus denitrificans (NBRC 12442) can grow on several primary amines as a sole source of carbon, nitrogen and energy. To date, two kinds of quinoprotein amine dehydrogenases have been discovered as the primary enzymes of the amine oxidation, methylamine dehydrogenase (MADH) (*1*) and quinohemoprotein amine dehydrogenase (QH-AmDH) (*2*). These enzymes are expressed when the organism is grown on methylamine or longer chain amines such as *n*-butylamine, respectively. Both enzymes catalyze the oxidation of amines to yield the corresponding aldehydes and ammonia. The physiological electron acceptor is amicyanin (a typical Type I copper protein) for MADH (*3*), but cytochrome c_{550} for QH-AmDH (*4*).

MADH is a $\alpha_2\beta_2$ structure protein, and contains a covalently bound organic cofactor tryptophan tryptophylquinone (TTQ) in each of the β subunits, while the larger α subunit does not possess any prosthetic groups (*5*). The redox potential (strictly formal potential, $E^{\circ\prime}$) of MADH have been reported as 0.100 V (*6*) or 0.130 V (*7*) at pH 7.5. The structure of the MADH/amicyanin complex has been well elucidated (*8*) and the electron transfer kinetics from MADH to amicyanin has been also studied (*9*). These works demonstrate the significance of the hydrophilic property in the interaction between MADH and amicyanin (*8*). An enzyme closely similar to MADH is produced in *Alcaligenes faecalis* called aromatic amine dehydrogenase (*10, 11*).

QH-AmDH is a αβγ heterotrimeric protein, and has a novel covalently bound cofactor, cysteine tryptophylquinone (CTQ), in the smallest γ subunit and two hemes *c* in the largest α subunit, while the β subunit has not any redox center (*12*). One of heme *c* (named by heme *c* (a)) has His and Met as the first and second axial ligands, respectively, and is solvent accessible. The other heme *c* (named by heme *c* (b)) has *bis*-His axial ligands, and is partially buried and locates between CTQ and heme *c* (b) (*12*). The redox potential ($E^{\circ\prime}$) of these three cofactors, CTQ, heme *c* (b), and heme *c* (a), have been determined to be 0.065 V, 0.149, and 0.235 V, respectively, at pH 7.5 in my previous study (13). Another quinohemoprotein amine dehydrogenase (*14,15*) from *Pseudomonas putida* has a structure closely similar to that of

QH-AmDH (*16*). The electron transfer kinetics from QH-AmDH to cytochrome c_{550} has been reported, but details of the electron transfer from QH-AmDH to cytochrome c_{550} and other metalloproteins remain to be elucidated.

In the present study, the author attempted to compare cytochrome c_{550} with other related metalloproteins as electron acceptors of QH-AmDH from the kinetic viewpoints. Reconstitution of the respiratory chain was also examined. The electron acceptor specificity of QH-AmDH is discussed in view of thermodynamics and structural features.

EXPERIMENTAL PROCEDURES

Protein and related samples. QH-AmDH (*2,4*), MADH (*1*), cytochrome c_{550} (*4,17*), and amicyanin (*3*) from *P. denitrificans* were purified, and the concentration was determined according to the literature. Cytochrome *c* form horse heart was purchased from Sigma and used without further purification, of which the concentration was determined using the absorption coefficient at 550 nm (ε_{550} = 27600 M^{-1} cm^{-1} (*18*)). The oxidized and reduced forms of these proteins were prepared by adding $Fe(CN)_6^{3-}$ and solid $Na_2S_2O_4$, respectively. Cytoplasmic membrane fraction of *P. denitrificans* was prepared according to the literature (*4,15*).

Electrochemical measurements. Cyclic voltammetry and constant potential amperometry were performed with a Hokuto Denko (Japan) HZ-3000 potentiostat using an Ag/AgCl/KCl (sat.) reference electrode and a Pt-disk counter electrode. A thiol-modified Au working electrode was prepared as follows. An Au electrode (i.d. 1.6mm) (Bioanalytical Systems) was polished with alumina powder and sonicated in distilled water for about 15 min. The electrode was dipped into a saturated solution of *bis*-(4-pyridyl)disulfide (Sigma) for more than 30 min and washed thoroughly with distilled water. The electrochemical measurements were performed under anaerobic conditions at 25 °C and in 10 mM potassium phosphate buffer (pH 7.5, the ionic strength = 0.1 M with KCl). All redox potentials in this paper are referred to the standard hydrogen electrode (SHE) unless otherwise stated.

The respiratory activity of reconstituted respiratory chain was measured by monitoring

dioxygen consumption with a Clark-type oxygen electrode (Oriental Electric, Japan). Constant potential amperometry was performed at –400 mV vs. Ag/AgCl/KCl (sat) at 25 °C and in 10 mM potassium phosphate buffer (pH 7.5, the ionic strength = 0.1 M with KCl).

Other measurements. UV-visible absorption spectroscopy was recorded with a Shimadzu UV-1500PC spectrophotometer with micro quartz cells of the volume of 0.3 cm^3 and a light pass length of 1 cm. All experiments were performed at room temperature in 10 mM potassium phosphate buffer (pH 7.5, the ionic strength = 0.1 M with KCl). Isoelectronic focusing assay was performed with a Bio-Rad Mini IEF Cell.

RESULTS AND DISCUSSION

Steady-state enzyme kinetics between redox enzyme(s) and (first or second) substrate(s) can be easily evaluated by using the principle of mediated bioelectrocatalysis (*19–21*). This method has several advantages over the conventional spectrophotometric analysis. This is applicable to cases with the spectral overlapping between enzymes and substrates, and cases with low Michaelis constants and/or low absorption coefficients of substrate, and requires only very small amounts of samples (*4, 19–21*), although the substrate to be investigated must undergo reversible (or quasi-reversible) electrode reaction.

Amicyanin exhibited a pair of the cathodic and anodic waves in cyclic voltammetry at *bis*-(4-pyridyl)disulfide-modified electrode (broken line in Fig.1). The peak separation was 60 mV at least up to the scan rate (v) of 50 mV s^{-1}, and the peak currents were proportional to $v^{1/2}$, indicating the reversible one-electron characteristics. The modification of Au electrode with *bis*-(4-pyridyl)disulfide is essential for amicyanin to communicate with the electrode, where *bis*-(4-pyridyl)disulfide works as a promoter to accelerate the heterogeneous electron transfer kinetics (*21*). The $E^{\circ\prime}$ value was 0.234 V, which was evaluated as the midpoint potential of the cathodic and anodic peak potentials. This is slightly more negative than the reported value (0.294 V, (*23*)). Similar reversible voltammograms were obtained for cytochrome c_{550}, and horse heart cytochrome *c* at the thiol-modified electrode (data not shown), while the $E^{\circ\prime}$ values were 0.245, and 0.255 V, respectively, and close to those of the reported values (0.243 V at pH

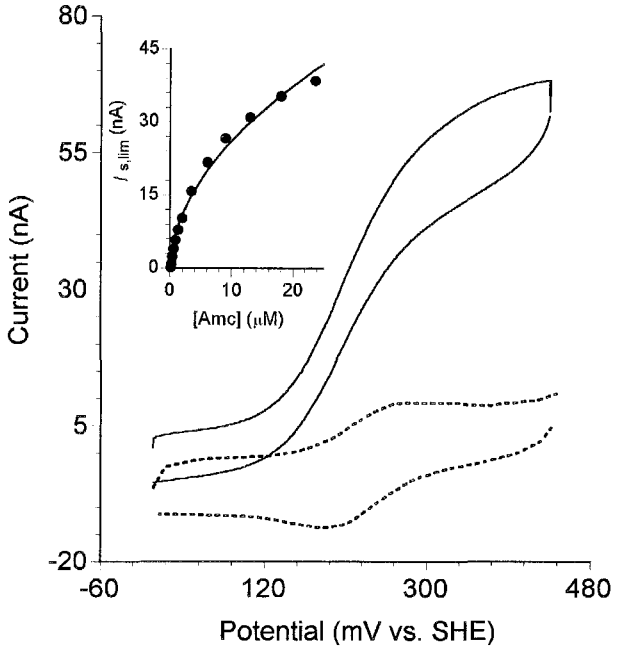

FIGURE 1: Cyclic voltammograms of 26 μM amicyanin in the absence (broken line) and presence (solid line) of 2.5 μM QH-AmDH and 20 mM *n*-butylamine at $v = 5$ mV s^{-1} in 10 mM potassium phosphate buffer (pH 7.5, the ionic strength = 0.1 M with KCl). The inset shows the dependence of the limiting catalytic current ($i_{s,lim}$) on the amicyanin concentration [Amc]. Solid curve represents the nonlinear regression results (see text).

7.5, (4); 0.255 V at pH 7.0 (*24*), respectively).

In contrast, QH-AmDH did not give any redox signal at the thiol-modified electrode, and the presence of QH-AmDH did not affect the voltammogram of amicyanin. When *n*-butylamine was added to the solutions as the (first) substrate of QH-AmDH, the voltammogram changed to typical catalytic characteristics, and the steady-state anodic current reached a limiting value ($i_{s,lim}$) at E more positive than $E°'$ of amicyanin (solid line in Fig.1). This is a bioelectrocatalytic oxidation of *n*-butylamine, where amicyanin works as a mediator to transfer the electron from the substrate-reduced QH-AmDH to the electrode. This means that amicyanin functions as a good electron acceptor of QH-AmDH.

The value of $i_{s,lim}$ increased with an increase of the concentration of amicyanin, as shown in the inset of Figure. Such curved characteristics of mediated bioelectrocatalysis can be given by (*21*):

$$\frac{I_{s,lim}}{FA} = \sqrt{2n_S n_M D_M k_{cat} K_M [E]\left[\frac{[M]^*}{K_M} - \ln\left(1+\frac{[M]^*}{K_M}\right)\right]} \quad (9)$$

under the conditions that the concentration of the first substrate (*n*-butylamine in this case) is sufficiently larger than the Michaelis constant for the substrate; that is, the steady-state kinetics (v_M)of the enzymatic reduction of the mediator (amicyanin in this case) at the length x from the electrode is given by:

$$v_M(x) = \frac{(n_S / n_M)k_{cat}[E]}{1 + K_M / [M_{ox}(x)]} \quad (10)$$

where k_{cat} and K_M are the catalytic rate constant and the Michaelis constant for the oxidized mediator, respectively. [E] and $[M]^*$ are the total concentration of the enzyme and the mediator,

Table 1. Steady-state enzyme kinetics of (A) QH-AmDH and (B) MADH with electron acceptor proteins and some thermodynamic parameters of the proteins.

Electron acceptor	k_{cat} (s^{-1}) [a]	K_M (μM) [a]	k_{cat}/K_M [a] (10^7 $M^{-1}s^{-1}$)	$E°'$ (mV)	p*I*
(A) **QH-AmDH** (p*I* = 4.2)					
Amicyanin	2.1	0.12	1.8	235	4.8 [b]
Cytochrome c_{550}	4.7 [c]	≤ 0.1 [c]	≥ 4.7 [c]	245	4.5 [d]
Horse heart cytochrome *c*	6.9	≤ 0.1	≥ 6.9	255	10.1
(B) **MADH** (p*I* = 4.3)					
Amicyanin	6.2 18 [e]	0.79 0.22 [e]	0.78 81 [e]	235	4.5 [b]
Cytochrome c_{550}	≈ 0.04 [f]	≈ 100 [f]	≈ 0.00004 [f]	245	4.5 [d]
Horse heart cytochrome *c*	nd [g]	nd [g]	nd [g]	255	10.1

a) Kinetic parameters were obtained on the basis of the theory of mediated bioelectrocatalysis unless otherwise stated.

b) The data taken from Ref. (3).

c) The related data reported in Ref. (4) were corrected in this work.

d) The data taken from Ref. (17).

e) The data taken from Ref. (9), which were determined by spectrophotometric method.

f) Catalytic current was not detected. The data were obtained by spectrophotometric method monitoring the decrease in the cytochrome c_{550} concentration at 550 nm.

g) Catalytic current not detected.

respectively, while $[M_{ox}(x)]$ is the concentration of the oxidized mediator at x; D_M is the diffusion coefficient of the mediator; n_s and n_m are the number of the electron of the first substrate and the mediator, respectively ($n_S = 2$, and $n_M = 1$ in this case), and A is the surface area of electrode. The values of k_{cat} and K_M were evaluated as 2.1 s^{-1}, and 1.2 $\times$ 10^{-7} M, respectively, by the non-linear regression analyses of the $i_{s,lim}$ vs. [amicyanin] profile (the inset of Figure).

Such catalytic waves were observed in the system containing cytochrome c_{550} (*4*) and also horse heart cytochrome *c* in place of amicyanin (data not shown). This means that QH-AmDH exhibits broad specificity against the electron acceptors, and that amicyanin and horse heart cytochrome *c* can work as a good electron acceptor, although cytochrome c_{550} is the physiological electron acceptor (*4*). The enzymatic kinetic parameters seem to be independent of the $E^{\circ\prime}$ and the isoelectric point (p*I*) of the electron acceptor, as summarized in Table 1.

In contrast, when MADH is used as an enzyme (and methylamine as the first substrate), a well-defined catalytic wave was observed only when amicyanin was present (data not shown), which is the physiological electron acceptor of MADH (*3*) (Table 1). Cytochrome c550 and horse heart cytochrome c did not work as an mediator. This means that MADH has high specificity toward amicyanin, which is in accord with the previous report (*8*). The specificity is also difficult to interpret in terms of $E^{\circ\prime}$ and/or p*I* of the metalloproteins.

It has been revealed that amicyanin or horse heart cytochrome *c* functions as a good electron acceptor of QH-AmDH, although constitutive cytochrome c_{550} is considered to be the physiological electron acceptor (*4*). This is in marked contrast with MADH, which shows high specificity to amicyanin (*3,17*). $E^{\circ\prime}$ and p*I* are not important factors in governing the electron acceptor specificity of QH-AmDH and MADH (Table 1). The electron donating-site of MADH is hydrophobic and convenient to interact with hydrophobic amicyanin, as has been pointed out already (*8*).

Cytochrome c_{550} and horse heart cytochrome *c* are rather hydrophilic proteins (*25*), and the surface circumstance near heme *c* (a) in QH-AmDH is hydrophilic (*12*). In addition, the electron transfer from heme *c* (a) to these cytochromes are thermodynamically favorable as judged from the $E^{\circ\prime}$ values. These profiles also support the electron transfer pathway from the

substrate to CTQ, heme *c* (b), heme *c* (a) and to cytochrome c_{550}. However, this idea is not adequate to explain why hydrophobic amicyanin with $E^{\circ\prime}$ slightly more negative than that of heme *c* (a) can act as a good electron acceptor of QH-AmDH. Therefore, the electron donating site to amicyanin may be heme *c* (b), which exits in a hydrophobic environment (*12*) and has $E^{\circ\prime}$ more negative than that of amicyanin.

For the physiological couples of the enzyme and the electron acceptor, the bimolecular reaction rate constants (k_{cat}/K_M) are in the range expected for the diffusion-controlled kinetics of proteins (*26*). The fact that both K_M values of QH-AmDH-cytochrome c_{550} and MADH-amicyanin couples are in the order of μM is consistent with the fact that these electron transfer proteins (cytochrome c_{550} and amicyanin) exist *in vivo* at very low concentrations (*27*).

In this work, the author also reconstituted the amine oxidation respiratory chain in order to ensure whether amicyanin and horse heart cytochrome *c* work as electron-transfer proteins from QH-AmDH and the terminal oxidase in the cytoplasmic membrane.

Enhancement of dioxygen consumption was observed on the addition of amicyanin or horse heart cytochrome *c* into a cytoplasmic membrane suspension containing QH-AmDH and *n*-butylamine, as in the case of the physiological acceptor, cytochrome c_{550} (*4*). The kinetic data of the dioxygen uptake in the reconstituted systems are summarized in Table 2, which also includes the data of the MADH system containing amicyanin and cytochrome c_{550}. Interestingly, horse heart cytochrome *c* works better than cytochrome c_{550} as an

Table 2. Rate of dioxygen uptake in the reconstituted respiratory chain of the amine oxidation in *Paracoccus denitrificans*

primary enzyme + substrate	electron-transfer protein	O_2 uptake rate (nM s^{-1})
QH-AmDH (3.0 μM) + *n*-butylamine (6.5 mM)	cytochrome c_{550} (1.3 μM)	130
	amicyanin (5.5 μM)	100
	horse heart cytochrome *c* (1.0 μM)	300
MADH (3.3 μM) + methylamine (6.7 mM)	amicyanin (5.5 μM) + cytochrome c_{550} (1.3 μM)	150

a) The measurements were done in the presence of cytoplasmic membrane suspension (0.4 mg protein mL^{-1}) at pH 7.5.

electron-transfer protein for QH-AmDH.

Amicyanin is induced together with MADH (*28*), and the production was not detected when *P. denitrificans* was grown on *n*-butylamine (*4*). However, QH-AmDH is slightly induced as well as MADH in *P. denitrificans*, when grown on high concentrations of methylamine as a carbon source (*2*). Under such conditions, there should be two electron acceptors of QH-AmDH in the cytoplasm, cytochrome c_{550} and amicyanin. The electron transfer from amicyanin to the terminal oxidase may occur through various pathways to construct an electron-transfer network (*29–31*). Therefore, both cytochrome c_{550} and amicyanin play an important role as key electron transfer proteins in the metabolism of amines.

The fact that horse heart cytochrome *c* works as a good electron transfer proteins is not important in biological meaning. However, it is useful and convenient to construct a histamine sensor. Previously, the author constructed a QH-AmDH-based amperometric histamine sensor (*32*), in which cytochrome c_{550} was used as a good electron-transfer mediator between QH-AmDH and thiol-modified electrodes. The present work has revealed that cytochrome c_{550} can be replaced with horse heart cytochrome *c*, which is commercially available. Improvement of the QH-AmDH-based histamine sensor is in progress.

SUMMARY

Paracoccus denitrificans produces two primary enzymes for the amine oxidation, tryptophan tryptophylquinone-containing methylamine dehydrogenase and quinohemoprotein amine dehydrogenase. QH-AmDH has a novel cofactor, cysteine tryptophylquinone and two hemes *c*. In this work, kinetics of the electron transfer from QH-AmDH to three kinds of metalloproteins, amicyanin, cytochrome c_{550}, and horse heart cytochrome *c* were examined on the basis of the theory of mediated-bioelectrocatalysis. All these metalloproteins work as a good electron acceptor of QH-AmDH and donate the electron to the terminal oxidase of *P. denitrificans*, which was revealed by reconstitution of the respiratory chain. These properties are in marked contrast with those of MADH, which shows high specificity to amicyanin. These electron transfer kinetics are discussed in terms of thermodynamics and structural

property.

REFERENCES

1. Husain, M. and Davidson, V.L. (1987) *J. Bacteriol. 169*, 1712–1717.
2. Takagi, K., Torimura, M., Kawaguchi, K., Kano, K., and Ikeda, T. (1999) *Biochemistry 38*, 6935–6942.
3. Husain, M., and Davidson, V.L. (1985) *J. Biol. Chem. 260*, 14626–14629.
4. Takagi, K., Yamamoto, K., Kano, K., and Ikeda, T. (2001) *Eur. J. Biochem. 268*, 470–476.
5. McIntire, W.S., Wemmer, D.E., Chistoserdov, A., and Lidstrom, M.E. (1991) *Science 252*, 817–824.
6. Husain, M., and Davidson, V.L. (1987) *Biochemistry 26*, 4139–4143.
7. Sato, A., Torimura, M., Takagi, K., Kano, K., and Ikeda, T. (2000) *Anal. Chem. 72*, 150–155.
8. Chen, L. Durley, R., Poliks, J.B., Hamada, K. Chen, Z. Mathews, F.S., Davidson, V.L., Satow, Y., Huizinga, E., Vellieux, F.M.D., Hol, W.G.J. (1992) *Biochemistry 31*, 4959–4964.
9. Davidson, V.L. and Jones, L.H. (1991) *Anal. Chim. Acta 249*, 235–240.
10. Iwaki, M., Yagi, T., Horiike, K. Saeki, Y., Ushijima, T., and Nozaki, M. (1983) *Arch. Biochem. Biophys. 220*, 253–262.
11. Govindaraj, S., Eisenstein, E., Jones, L.H., Sanders-Leohr, J., Chistoserdov, A.Y., Davidson, V.L., and Edwards, S.L. (1994) *J. Bacteriol. 176*, 2922–2929.
12. Datta, S. Mori, Y. Takagi, K., Kawaguchi, K., Chen, Z., Okajima, T., Kuroda, S., Ikeda, T., Kano, K., Tanizawa, K., and Mathews, F.S. (2001) *Proc. Natl. Acad. Sci. U.S.A. 98*, 14268–14273.
13. Fujieda, N., Mori, M., Kano K., and Ikeda, T. (2002) *Biochemistry 41*, 13736–13743.
14. Shinagawa, E., Matsushita, K., Nakashima, K., Adachi, O., and Ameyama, M. (1988) *Agric. Biol. Chem. 52*, 2255–2263.
15. Adachi, O., Kubota, T., Hacisalihoglu, A., Toyama, H., Shinagawa, E., Duine, J.A., and Matsushita, K. (1998) *Biosci. Biotechnol. Biochem. 62*, 469–478.

16. Satoh, A., Kim, J.K., Miyahara, I., Devreese, B., Vandenberghe, I., Hacisalihoglu, A., Okajima, T., Kuroda, S., Adachi, O. Duine, J.A. Van Beeumen, J., Tanizawa, K., and Hirotsu, K. (2002) *J. Biol. Chem. 277*, 2830–2834.
17. Husain, M. and Davidson, V.L. (1986) *J. Biol. Chem. 261*, 8577–8580.
18. Margoliash, E., and Frohwirt, N. (1959) *Biochem. J. 71*, 570–572.
19. Kano, K., Ohgaru, T., Nakase, H., and Ikeda, T. (1996) *Chem. Lett. 6*, 439–440.
20. Ohgaru, T., Tatsumi, H., Kano, K., and Ikeda, T. (2000) *J. Electroanal. Chem. 496*, 37–43.
21. Matsumoto, R., Kano, K., and Ikeda, T. (2002) *J. Electroanal. Chem. 535*, 37–40.
22. Hill, H.A.O. (1987) *Pure Appl. Chem. 59*, 743–748.
23. Gray, K.A., Knaff, D.B., Husain, M., Davidson, V.L. (1986) *FEBS Lett. 207*, 239–242.
24. Eddowes, M.J., Hill, H.A.O., (1979) *J. Am. Chem. Soc. 101*, 4461–4464.
25. Timkovich, R., and Dickerson, R.E. (1976) *J. Biol. Chem. 251*, 4033–4046.
26. K. Hiromi (Ed.), Kinetics of Fast Enzyme Reactions –Theory and Practice, Kodansha Ltd., Tokyo, 1979, pp. 255–286.
27. Itoh, S., Ogino, M., Haranou, S., Terasaka, T., Ando, T., Komatsu, M., Ohshiro, Y., Fukuzumi, S., Kano, K., Takagi, K., and Ikeda, T. (1995) *J. Am. Chem. Soc. 117*, 1485–1493.
28. Chistoserdov, A.Y., Boyd, J., Mathews, F.S., and Lidstrom, M.E. (1992) *Biochem. Biophys. Res. Commun. 184*, 1181–1189.
29. De Gier, J.W., Van der Oost, J., Harms, N., Stouthamer, A.H., and Van Spanning, R.J.M. (1995) *Eur. J. Biochem. 229*, 148–154.
30. Van der Oost, J., Schepper, M., Stouthamer, A.H., Westerhoff, H.V., Van Spanning, R.J.M., and De Gier, J.-W.L. (1995) *FEBS Lett. 371*, 267–270.
31. Otten, M.F., Van der Oost, J., Reijnders, W.N., Westerhoff, H.V., Ludwig, B., and Van Spanning, R.J.M. (2001) *J. Bacteriol. 183*, 7017–7026.
32. Yamamoto, K., Takagi, K., Kano, K., and Ikeda, T. (2001) *Electroanalysis 13*, 375–379.

1.3. Activation and Characterization of Silent Form Quinohemoprotein Amine Dehydrogenase from Paracoccus denitrificans

After the discovery of PQQ, many kinds of PQQ-containing enzymes have been discovered and identified. These discoveries were followed by the unorthodox finding of a protein-bound tyrosine-derived cofactor TPQ in an eukaryotic copper amine oxidase (*1*). This exciting discovery was also followed by the reports on a tryptophyl quinone cofactor which is cross-linked to a second tryptophan to form TTQ in methylamine dehydrogenase (*2*), and led to the finding of lysine tyrosyl quinone (LTQ) in lysyl oxidase (*3*), where a tyrosine-based quinone is cross-linked to lysine. Since the several variants formed from tryptophan as well as tyrosine were reported, the field of quinone cofactor has turned out to be rich in view of structure.

Quinohemoprotein amine dehydrogenase (QH-AmDH) is induced when *Paracoccus denitrificans* (*4*) and *Pseudomonas putida* (*5*, *6*) are grown on media including biological amines as the sole source of carbon, nitrogen, and energy. QH-AmDH is a soluble bacterial enzyme that catalyzes the oxidative deamination of amines to formaldehydes plus ammonia. Two groups have recently revealed the crystallographic structure of QH-AmDH from *P. denitrificans* and *P. putida*, respectively (*7*, *8*). QH-AmDH is a $\alpha\beta\gamma$ heterotrimeric protein and the smallest γ subunit has a novel quinone cofactor, in which a tryptophyl quinone is cross-linked to a cysteine to form cysteine tryptophylquinone (CTQ). This finding leads us to expect the discoveries of other unknown quinone cofactors.

It has previously been reported that *P. denitrificans* expresses four soluble hemoproteins predominantly when grown on media containing butylamine. One of those, designated as "heme 2" in the literature, showed two bands of molecular mass 59.5 kDa and 36.5 kDa on SDS/PAGE (*9*). This profile is almost identical with that of QH-AmDH, but heme 2 showed no QH-AmDH activity. In this study, the author attempted to characterize this hemoprotein.

EXPERIMENTAL PROCEDURES

Purification and preparations of QH-AmDH and heme 2. QH-AmDH and heme 2 from *P. denitrificans* were isolated and purified as described in the literature (*9*). The concentration of the reduced proteins was determined from the absorbance at 552 nm (ε=37.2 $mM^{-1}cm^{-1}$), respectively. The fully oxidized and reduced forms of QH-AmDH and heme 2 were prepared by adding $K_3Fe(CN)_6$ and *n*-butylamine (or $Na_2S_2O_4$), respectively. The γ subunits of QH-AmDH and heme 2 were isolated as previously reported (*10*).

Activation of heme 2 by reductants and oxidants. Activation of heme 2 was performed as follows. An aliquot of heme 2 solutions (24 μM) was mixed with appropriate amounts of amines or dithionite (10 mM) or dithiotreitol (35 mM) in 10 mM potassium phosphate (pH 7.5), and incubation at 30 °C in the case of amines. The samples were isolated and desalted using PD-10 gel filtration column (Amersham Co.). Steady-state kinetic assays for the QH-AmDH activity were performed spectrophotometrically by measuring the amine-dependent reduction rate of $Fe(CN)_6^{3-}$ at 417 nm and 30 °C. The reaction mixture contained $K_3Fe(CN)_6$ (1 mM) and *n*-butylamine (10 mM) in 0.1 M potassium phosphate (pH 7.5).

Mediator-Assisted Continuous-Flow Column Electrolytic Spectroelectrochemistry (MCES). MCES of heme 2 were performed as described in the literature (*10*). Potassium ferricyanide, 2,6-dimethylbenzoquinone, *N*-methylphenazinium methosulfate (PMS), phenazine ethosulfate (PES), vitamin K_3 and 2-hydroxy-1,4-napthoquinone ($E°'$ of these compounds at pH 7.0 being 0.443, 0.169, 0.08, 0.055, 0.009 and –0.139 V vs. SHE, respectively.) were used as mediators. A portion of a protein sample was injected on a mobile phase buffer (pH 7.0) and mixed with a mixed mediator solution on a two-channel flow injection system. The mixed mediator solution and a mobile phase buffer were thoroughly deaerated with argon gas and flowed at 0.35 mL min^{-1}. Other details of the principle, instruments, and methods are described in the literature (*11*, *12*).

Activation of heme 2 by column electrode was performed as follows. 2,6-dimethylbenzoquinone, indigotrisulfonate, 2-hydroxy-1,4-napthoquinone, anthraquinone-2-sulfonic acid, benzyl viologen and methyl viologen ($E°'$ of these compounds at pH 7.0 being

0.169, -0.080, –0.139, -0.249, -0.359 and –0.435V vs. SHE, respectively.) were separately used as mediators (25 μM). A portion of a protein sample (usually 5 μL and a order of 40 μM) was injected on a mobile phase buffer (0.1 M potassium phosphate pH 7.0) containing individual mediator on a one-channel flow injection system. The mediator solution were thoroughly deaerated with argon gas and flowed at 1.0 mL min^{-1}. All potential values are reported relative to the SHE, unless otherwise stated.

Preparations of QH-AmDH-hydroxylamine adduct. QH-AmDH hydroxylamine adduct were prepared as follows. An aliquot of full-oxidized QH-AmDH solutions (100 μM) was mixed with hydroxylamine (1 mM) in 10 mM potassium phosphate (pH 7.5) and incubation at 30 °C for 30 min. The samples were isolated and desalted using PD-10 gel filtration column (Amersham Co.).

Mass spectroscopy. The γ subunits of QH-AmDH and heme 2 were highly purified and desalted using STR-ODS reverse-phase column (Shimadzu Co.) pre-equilibrated with solvent A (0.1 % trifluoroacetic acid, H_2O) and eluted in a linear gradient with 0-50 % solvent B (0.08 % trifluoroacetic acid, acetonitrile) over 50 min. Purified sample was mixed with 10 % trichloroacetic acid and left in an ice bath for 15 min. The precipitate formed was washed with acetone several times and dissolved in solvent C (3 % acetic acid, 40 % acetonitrile, H_2O). The solution was injected into a quadrupole mass spectrometer API 165 (PerkinElmer Sciex)

RESULTS AND DISCUSSION

Heme 2 showed no enzymatic activity toward various amines. However, as incubated with butylamine, a substrate of QH-AmDH, heme 2 was slowly activated and showed QH-AmDH activity in several ten hours. The amount of activated enzyme depended on the concentration of butylamine as shown in Figure 1a. The activation rate was faster than the activation rate with methylamine, which is a poor substrate for QH-AmDH (Data not shown). In contrast, heme 2 was rapidly activated by the addition of ditihionite and dithiothreitol.

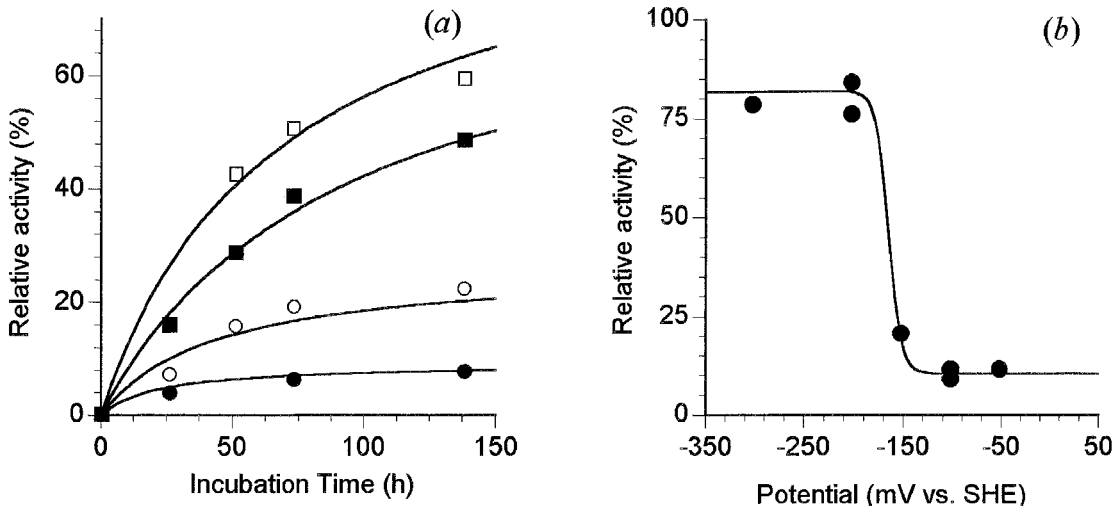

FIGURE 1: Activation of *s*QH-AmDH by the incubation with butylamine (*a*) and the mediated column electrolysis (*b*). (*a*) QH-AmDH activity after incuvation with various concentration of butylamine at 30°C. (●) 0.1 mM;(○) 1 mM;(■) 10 mM;(□) 100mM. (*b*) A portion of *s*QH-AmDH was injected on a mobile phase and mixed with an electrochemically regulated mediator solution. The electrolyzed mixtures were collected and analyzed QH-AmDH activity.

These results suggested that heme 2 was a silent form of quinohemoprotein amine dehydrogenase (*s*QH-AmDH; the letter "*s*" means the symbol of "silent".).

*s*QH-AmDH was not activated by direct electrolytic reduction with a column electrode at −0.5 V, but was activated by mediated electrolytic reduction with a column electrode. The dependence of QH-AmDH activity on the electrode potentials was shown in Figure 1b. Since the QH-AmDH activity sharply appeared within the range from –0.2 to –0.1 V, the activation potential of *s*QH-AmDH (E_{act}) can be determined to be ca. –0.17 V. It might expect that the reduction of disulfide bond was involved in this activation, because this value is close to that of thiol/disulfide couple. However, no disulfide bonds are formed in QH-AmDH (*7*).

The QH-AmDH activity remained practically unchanged in the potential regions from –0.05 to 0.1 V. The spectrum of *s*QH-AmDH showed the reduced form on the electrode potential from –0.05 to 0 V. From the result, it was likely that the redox reactions of two hemes *c* were not involved with the activation of *s*QH-AmDH. More details of spectral changes were analyzed by MCES as follows. QH-AmDH exhibited reproducible spectral changes depending on the electrode potential (*E*) at a flow rate of 0.35 ml min^{-1} at pH 7.0 (0.1

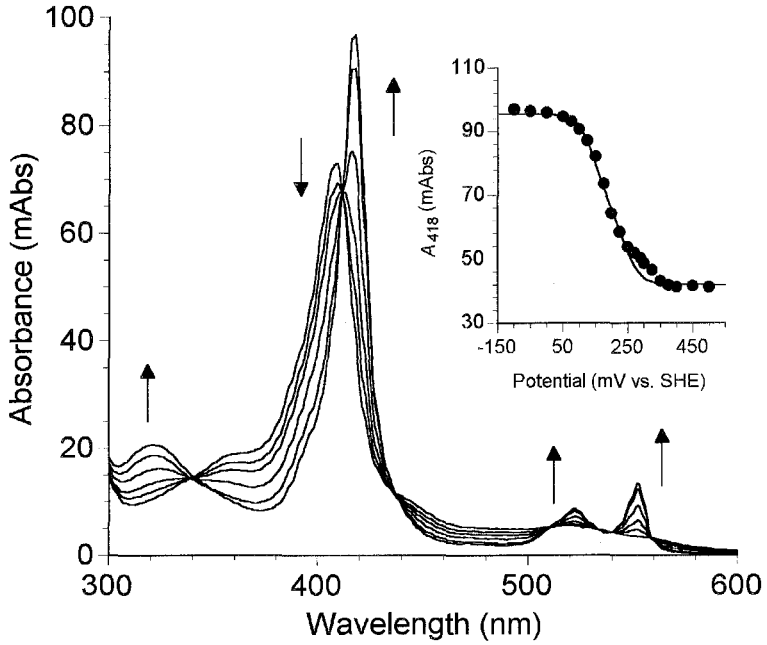

FIGURE 2: Background-corrected absorption spectra of QH-AmDH at 0.397 (fully oxidized), 0.297, 0.222, 0.172, 0.097 and –0.103 V (fully reduced) and at pH 7.0. An aliquot of fully oxidized QH-AmDH sample (40 μM × 10 μL) was injected at each electrode potential to an MCES system with a flow rate of 0.35 ml min^{-1}. Mediators used were 50 μM potassium ferricyanide, 125 μM 2,6-dimethylbenzoquinone, 20 μM *N*-methylphenazinium methosulfate (PMS), 10 μM phenazine ethosulfate (PES), 10 μM vitamin K_3, and 75 μM 2-hydroxy-1,4-napthoquinone. The arrows indicate the direction of the spectral changes on the reduction of QH-AmDH. Inset; Spectroelectrochemical titration curve of *s*QH-AmDH at 418 nm (A_{418}) under equilibrated conditions. (•) Experimental data; (–) nonlinear regression curve.

M potassium phosphate, ionic strength 0.3 M with KCl) in the presence of the mixed mediators (Figure 2). The spectral change is characteristic of the redox reaction of heme *c* groups. The absorption spectra obtained at 0.4 and –0.1 V were almost identical with those of the fully oxidized form (prepared by the oxidation with $K_3Fe(CN)_6$) and the fully reduced one (prepared by the reduction with $Na_2S_2O_4$), respectively. During the spectral change, the isosbestic points appeared at 342, 411, 440, 510, 538 and 561 nm. The spectra remained practically unchanged in the potential regions from –0.4 to –0.1 V and from 0.4 to 0.6 V. The *E* dependence of the absorbance at 418 nm (A_{418}) (depicted in Figure 2 inset) shows only one-step change. The redox potentials ($E^{\circ\prime}$) were determined as 0.237± 0.002 and 0.146±

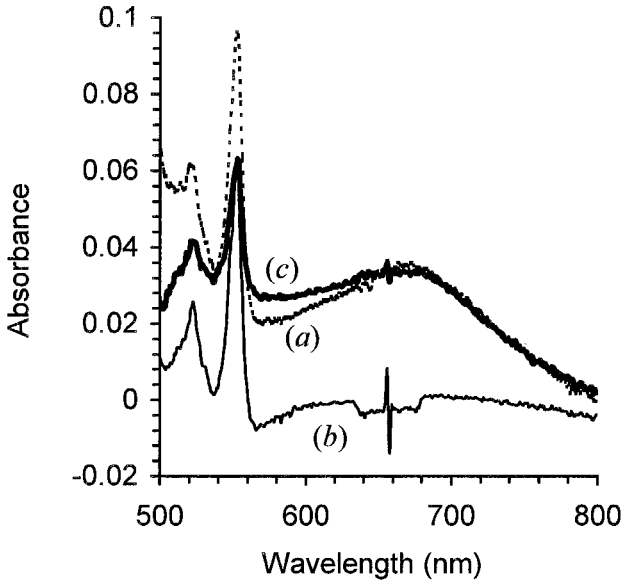

FIGURE 3: UV-vis spetra of CTQ-4-nitrophenylhydrazone of (*a*) QH-AmDH, (*b*) *s*QH-AmDH, (*c*) activated *s*QH-AmDH.

0.005 V by the analysis described previously, (*10*). The values were so far from E_{act}, but practically identical to those of QH-AmDH. These results suggested that reduction of the two hemes *c* were independent of the activation process.

In QH-AmDH, CTQ is the sole redox site except for the two hemes *c*. Qualitative analysis of quinone was performed to make sure the presence of CTQ, particularly the quinonone carbonyl groups, in *s*QH-AmDH. QH-AmDH has high reactivity to the carbonyl reagents such as phenylhydrazine and semicarbazide (*4*). Especially, the UV-vis spectrum of the corresponding hydrazones, which is formed by the reaction between CTQ and 4-nitrophenylhydrazine, shows a peak at 665 nm (*4*). 4-Nitrophenylhydrazine-treated *s*QH-AmDH didn't show such spectrum change, but the activated *s*QH-AmDH showed almost identical change (Figure 3) in absorption spectrum, indicating the hydrazone formation in the activated *s*QH-AmDH. These results suggested that the hydrazine-binding site of QH-AmDH, that is the carbonyl group of CTQ, is absent or blocked in *s*QH-AmDH.

For the purpose of the clarification of this difference, the properties of γ subunit of *s*QH-AmDH were compared with those of QH-AmDH. The UV-vis spectrum of γ subunit of *s*QH-AmDH showed a peak at 390 nm, and it was quite different from that of QH-AmDH

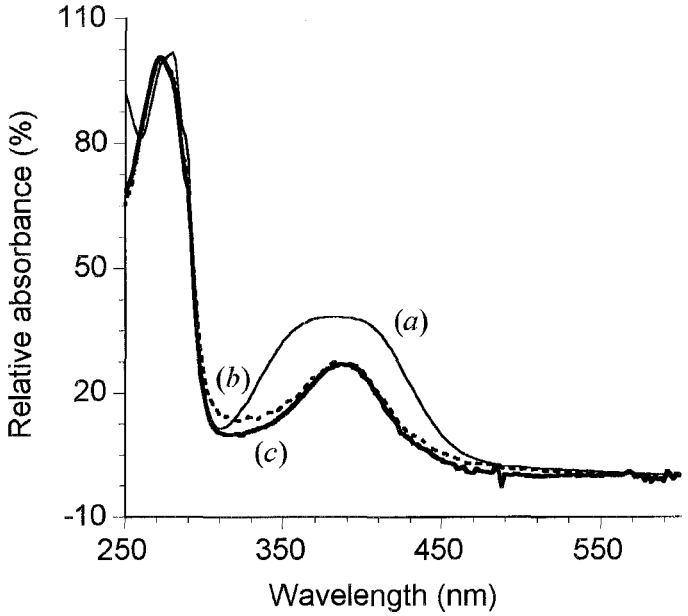

FIGURE 4: Normalized UV-vis spetra of γ subunit of (*a*) QH-AmDH, (*b*) *s*QH-AmDH, (*c*) hydroxylamine adduct of QH-AmDH.

(Figure 4ab). The molecular mass of γ subunit of *s*QH-AmDH and QH-AmDH were determined to be 8871.5 and 8856.4, respectively, by ESMS. The difference was 15.1 and this value is successfully assigned to the sum of mass numbers of nitrogen and hydrogen. This result may suggest the presence of CTQ-*6*-oxime or CTQ-7-oxime in *s*QH-AmDH.

The oxime was prepared by the reaction between hydroxylamine and QH-AmDH. The γ subunit of the hydroxylamine adduct of QH-AmDH was isolated in the same manner for *s*QH-AmDH. It showed a UV-vis spectrum very similar to that of *s*QH-AmDH (Figure 4c). In addition, the hydroxylamine adduct of QH-AmDH was slowly activated by butylamine. This is the behavior similar to that of *s*QH-AmDH. By considering the reactivity of the two carbonyl groups based on X-ray structural analysis of hydrazine adduct of QH-AmDH (*13*, *14*), this hydroxylamine adduct has CTQ-*6*-oxime (Figure 5). This oxime form has not been reported so far. This structure is very remarkable and unique as a chromophore, although it is not obvious whether the oxime form of CTQ function in enzyme catalysis.

It can be safely concluded that the reductive activation of *s*QH-AmDH is initiated by the direct reduction of CTQ-*6*-oxime. It seems that CTQ-*6*-oxime is converted to aminophenol via hydroxyaminophenol by a two-electron reduction on the respective steps. The

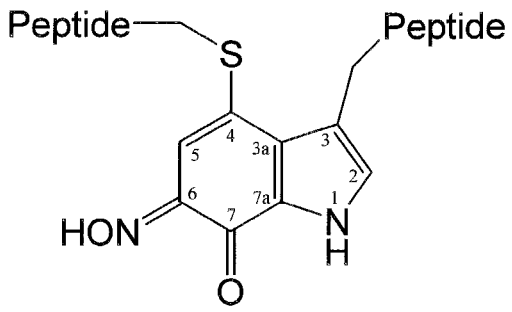

FIGURE 5. Structure of CTQ-*6*-oxime.

aminophenol, which is observed in the catalytic reaction of TTQ-containing amine dehydrogenase (*15*), may be hydrolysis and produce CTQ and ammonia. These reactions would occur by the substrate and biological reductants such as gultationedisulfide *in vivo*. On the other hands, *Nitrosomonas europaea* and *P. pantotropha* generate hydroxylamine in the process of nitrification and aerobic denitrification (*16*). *P. denitrificans* is closely-related species to *Paracoccus pantotropha* and might generate hydroxylamine (*17*). The hydroxylamine might react to QH-AmDH and block 6-carbonyl group of CTQ. However, amino acid modified quinone cofactors would be formed by post-transcriptional modification. Modification process of TPQ (*18*) and TTQ (*19-21*) has been reported, but that of CTQ remains still obscure. If *s*QH-AmDH is the precursor of QH-AmDH, *s*QH-AmDH must allow the author to obtain new discovery and to understand about post-transcriptional modification of quinone cofactors. The researches relevant to physiological roles of *s*QH-AmDH are in progress.

SUMMARY

Silent form of quinohemoprotein amine dehydrogenase was activated and characterized. The protein was slowly activated by substrates, butylamine and phenetylamine, and also activated immediately by reductants, dithionite and dithiothreitol. The protein didn't react to 4-nitrophenylhydrazine and its γ subunit has several properties different from those of

the native enzyme. UV-vis spectrum was different from that of the native enzyme and showed a peak at 390 nm. The molecular mass was larger than that of the native enzyme by 15.1. On the other hand, UV-vis spectral properties of the γ subunit of hydroxylamine-adduct from the native enzyme were identical to those of the silent form of quinohemoprotein amine dehydrogenase. This adduct was reactivated by substrate and reductant as is the case of the silent form.

REFERENCES

1. Janes, S. M., Mu, D., Wemmer, D., Smith, A. J., Kaur, S., Maltby, D., Burlingame, A. L. and Klinman, J. P. (1990) *Science 248*, 981–987.
2. McIntire, S., Wemmer, D. E., Christoserdov, A. Y. and Lidstrom, M. E. (1991) *Science 252*, 817–824.
3. Wang, S., Mure, M., Medzihradszky, K. F., Burlingame, A. L., Brown, D. E., Dooley, D. M., Smith, A. J., Kagan, H. M. and Klinman, J. P. (1996) *Science 273*, 1078–1084.
4. Takagi, K., Torimura, M., Kawaguchi, K., Kano, K., and Ikeda, T. (1999) *Biochemistry 38*, 6935–6942.
5. Shinagawa, E., Matsushita, K., Nakashima, K., Adachi, O., and Ameyama, M. (1998) *Agric. Biol. Chem. 52*, 2255–2263.
6. Adachi, O., Kubota, T., Hacisalihoglu, A., Toyama, H., Shinagawa, E., Duine, J. A., and Matsushita, K. (1998) *Biosci. Biotechnol. Biochem. 62*, 469–478.
7. Datta, S., Mori, Y., Takagi, K., Kawaguchi, K., Chen, Z., Okajima, T., Kuroda, S., Ikeda, T., Kano, K., Tanizawa, K., and Mathews, F. S. (2001) *Proc. Natl. Acad. Sci. U.S.A. 98*, 14268–14273.
8. Satoh, A., Kim, J., K., Miyahara, I., Devreese, B., Vandenberghe, I., Hacisalihoglu, A., Okajima, T., Kuroda, S., Adachi, O., Duine, J., A., Van Beeumen, J., Tanizawa, K., and Hirotsu, K. (2002) *J. Biol. Chem. 277*, 2830–2834.
9. Takagi, K., Yamamoto, K., Kano, K., and Ikeda, T. (2001) *Eur. J. Biochem.* 268, 470–476.
10. Fujieda, N., Mori, M., Kano K., and Ikeda, T., (2002) *Biochemistry 41*, 13736 –13743.
11. Torimura, M., Mochizuki, M., Kano, K., Ikeda, T., and Ueda, T. (1998) *Anal. Chem. 70*,

4690–4695.

12. Sato, A., Torimura, M., Takagi, K., Kano, K., and Ikeda, T. (2000) *Anal. Chem. 72*, 150–155.
13. Datta, S., Ikeda, T., Kano, K., and Mathews, F. S. (2003) *Acta Crystallogr. D 59*, 1551–1556.
14. Satoh, A., Adachi, O., Tanizawa, K., and Hirotsu Ken. (2003) *Biochim. Biophys. Acta 1647*, 272–277.
15. Davidson, V. L., Jones, L. H., Graichen, M. E., (1992) *Biochemistry 31*, 3385–3390.
16. Jetten, M. S. M., Logemann, S., Muyzer, G., Robertson, L. A., De Vries, S., Van Loosdrecht, M. C. M., Kuenen, J. G., (1997) *Antonie van Leeuwenhoek 71*, 75–93.
17. Stouthamer, A. H., De Boer, A. P. N., Van Der Oost, J., Van Spanning, R. J. M., (1997) *Antonie van Leeuwenhoek 71*, 33–41.
18. DuBois, J. L. and Klinman, J. P., (2005) *Arch. Biochem. Biophys. 433*, 255–265.
19. Jones, L. H., Pearson, A. R., Tang, Y., Wilmot, C. M., and Davidson, V. L. (2005) *J. Biol. Chem. 280*, 17392–17396.
20. Wang, Y., Li, X., Jones, L. H., Pearson, A. R., Wilmot, C. M., and Davidson V. L., (2005) *J. Ameri. Chem. Soc. 127*, 8258–8259.
21. Pearson, A. R., De la, M.-R. T., Graichen, M. E., Wang, Y., Jones, L. H. Marimanikkupam, S., Agger, S. A., Grimsrud, P. A., Davidson, V. L., Wilmot, C. M., (2004) *Biochemistry 43*, 5494–5502.

CHAPTER 2

Histamine Dehydrogenase from *Nocardioides simplex*

2. 1. 6-S-Cysteinyl Flavin Mononucleotide-Containing Histamine Dehydrogenase from Nocardioides simplex: Molecular Cloning, Sequencing, Overexpression, and Characterization of Redox Centers of Enzyme

Histamine is one of the most significant bioactive amines, playing a key role in the regulation of several physiological processes, and is recognized in high specificity by various proteins. Although several efforts have been devoted to understanding the mode of its binding with various proteins from physiological and pharmacological viewpoints (*1*), details remain still obscure. Recently, histamine dehydrogenase (HmDH) has been discovered from *Nocardioides simplex*, one of Gram-positive actinobacteria (*2, 3*). The enzyme is a homodimer and highly specific to histamine, and catalyzes the oxidative deamination of histamine to imidazole acetaldehyde:

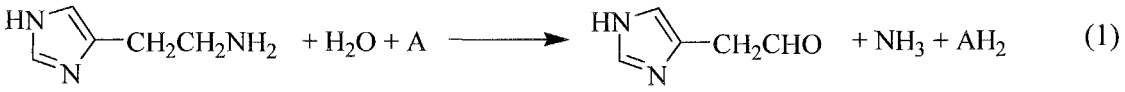

(1)

where A and AH_2 are a two-electron acceptor (or two moles of one-electron acceptor) and its reduced form, respectively. It was suggested that HmDH contained a covalently bound organic cofactor, which was expected to be a quinone-like compound on the basis of its absorption spectra and the positive staining in quinone-dependent redox cycling (*2*).

Two kinds of quinoprotein primary-amine dehydrogenases have been discovered to date from some Gram-negative bacteria. These enzymes catalyze the following reaction:

$$RCH_2NH_2 + H_2O + A \rightarrow RCHO + NH_3 + AH_2 \quad (2)$$

One group includes methylamine dehydrogenase from *Paracoccus denitrificans* (*4*) and aromatic amine dehydrogenase from *Alcaligenes faecalis* (*5*). These enzymes possess $\alpha_2\beta_2$ subunit structure and one covalently bound tryptophan tryptophylquinone as a prosthetic group in each β subunit (*6, 7*). The other group includes quinohemoprotein amine

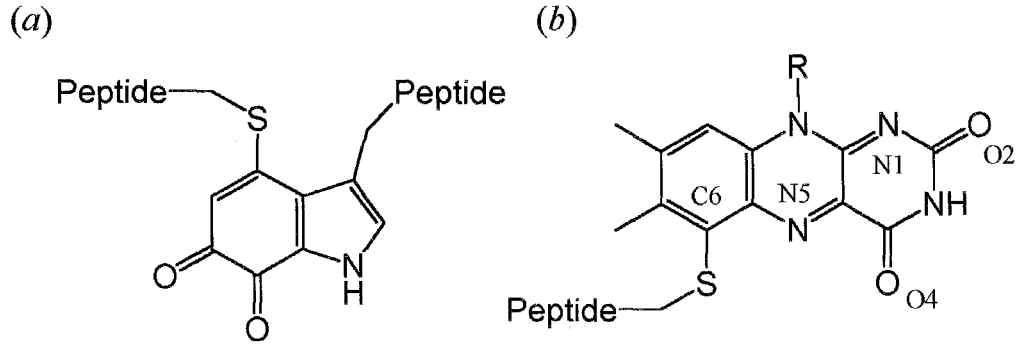

FIGURE 1: Structures of (*a*) cysteine tryptophylquinone and (*b*) 6-*S*-cysteinyl-flavin mononucleotide.

dehydrogenase (QH-AmDH) from *Pseudomonas putida* (*8*) and *Paracoccus denitrificans* (*9*). QH-AmDH consists of a heterotrimer and bears two hemes *c* in the largest subunit and one covalently bound cysteine tryptophylquinone (CTQ) in the smallest subunit as the redox active prosthetic group (Fig. 1a) (*10, 11*).

Another class of amine dehydrogenases is trimethylamine dehydrogenase (TMADH) from *Methylophilus methylotrophus* W_3A_1 and *Hyphomicrobium X* (*12*) and dimethylamine dehydrogenase (DMADH) from *Hyphomicrobium X* (*13*). These enzymes catalyze oxidative *N*-demethylation of tertiary and secondary amines:

$$RN(CH_3)_2 + H_2O + A \rightarrow RNH(CH_3) + HCHO + AH_2 \qquad (R = CH_3 \text{ or } H) \qquad (3)$$

TMADH and DMADH have a homodimeric structure; each subunit bears a 4Fe-4S cluster (*14*) and an unusual covalently bound flavin mononucleotide (FMN), 6-*S*-cysteinyl-FMN (Fig. 1b) (*15-17*). The primary structures of these two enzymes have been determined and are in a close relationship (63% identical) with each other, indicating that the enzymes are structurally homologous (*18, 19*). The crystal structure of TMADH has been solved at 2.4-Å resolution (*20*). Crystal analyses of TMADH soaked in a substrate inhibitor tetramethylammonium chloride solution or in a substrate trimethylamine solution revealed that these quaternary and tertiary ammonium ligands are accommodated in an "aromatic bowl" consisting of three residues: Tyr60, Trp264, and Trp355 (TMADH numbering) (*21*). The molecular modeling analysis of DMADH based on the crystal structure of TMADH indicated that both active site architectures are almost identical (*22*). The model demonstrated that a single amino acid

substitution (Tyr60 → Gln60) is responsible for the switch in substrate specificity in these two amine dehydrogenases. Several TMADH mutants were isolated by conventional site-directed mutagenesis and kinetic study with the mutants revealed some reasons why DMADH binds secondary alkylammonium ion preferentially over tertiary alkylammonium ion (*23*).

In this study, the author has clarified the primary structure of HmDH from *N. simplex* by PCR methods and over-expressed HmDH successfully in *Escherichia coli*. The amino acid sequence is highly correlated with those of TMADH and DMADH. This result suggests the presence of 6-*S*-cysteinyl-FMN and 4Fe-4S cluster as the redox centers in HmDH, and the expectation was verified by chemical and spectroscopic analyses. Moreover, sequence alignment study of the three 6-*S*-cysteinyl-FMN-containg enzymes and molecular modeling study based on the crystal coordinates of TMADH were performed for better understanding of the catalytic center, particularly the substrate binding site cavity.

EXPERIMENTAL PROCEDURES

Enzyme Purification. The culture conditions of *N. simplex* NBRC 12069 and the purification of HmDH were almost the same as described in a previous report (*2*) with some modifications. The cell-free extract was charged on a DEAE–Sepharose column (Amersham), equilibrated with 0.01 M potassium phosphate, pH 7.5, and eluted with a linear gradient of the buffer containing 0 M – 0.5 M NaCl. The final purification step was accomplished on a column of Hiload 26/60 Superdex 200 pg (Amersham) equilibrated with 0.05 M sodium phosphate, pH 7.5 containing 0.15 M NaCl. QH-AmDH from *P. denitrificans* was purified as described in the literature (*9*) and used as a reference enzyme in electron spin paramagnetic resonance spectroscopy (EPR).

Protein Sequencing and Mass Spectroscopy of HmDH. Automated Edman degradation was performed on a protein sequencer Procise 492 (Applied Biosystems), and electrospray ionization mass spectroscopy (ESMS) were done on a quadrupole mass spectrometer API 165 (PerkinElmer Sciex). For these measurements, HmDH samples were further purified and desalted using an Asahipak C4P C_4 reverse-phase column (Shodex) pre-equilibrated with

solvent A (0.1 % trifluoroacetic acid, H_2O) and eluted with linear gradient of 5–80 % solvent B (0.08 % trifluoroacetic acid, acetonitrile) over 30 min at 40 °C. The highly purified sample was analyzed as soon as possible (within 24h) with ESMS spectroscopy. In order to obtain internal amino acid sequences, HmDH was precipitated at 0 °C by addition of trichloroacetic acid to a final concentration of 5% (w/v). After centrifugation, the precipitate was re-suspended in 0.1 M Tris-HCl buffer at pH 8.1. Trypsin and chymotrypsin were added in a ratio of 1:50 (w/w) against HmDH. The tryptic and chymotryptic peptides were separated on a Symmetry 300 Å C_{18} reverse-phase column (Waters Co.).

Cloning and sequence determination of the hmd gene. Chromosomal DNA from *N. simplex* was prepared with an AquaPure Genomic DNA Isolation Kit (Bio-rad). In order to clone and sequence the *hmd* gene, degenerated oligonucleotide primers were designed based on the N-terminal and the internal amino acid sequences as (5'-CGA(C/T)GT(C/G/T)CT(C/G)TTCGA(A/G)CC(A/T/G/C)GT(C/G/T)CAGATCGG-3' and 5'-CTTGTT(A/C/G)GG(C/G)AGGAA(A/T/G/C)GG(A/G)TC-3'). An about 1-kbp portion of the *hmd* gene was amplified from genomic DNA of *N. simplex* by polymerase chain reaction (PCR) with these degenerated primers and Taq polymerase (Promega). The conditions of the amplification (30 cycles) were as follows: denaturation 94 °C (30 s), annealing 55 °C (30 s), and extension 73 °C (90 s). After purification on agarose gels, the fragments were ligated in pGEM-T EASY Vector, a TA cloning vector, for preliminary sequencing. Recommendations of the manufacturer (Promega) are followed in all manipulations of the plasmid and conditions for ligation. *Escherichia coli* JM109 cells were transformed with the ligated plasmid according to the literature (*24*). Three fragments of about 0.4 kbp, 0.7 kbp and 2.5 kbp were amplified by the thermal asymmetric interlaced PCR (TAIL-PCR) method with a shorter arbitrary degenerated primer (5'-(A/T/G/C)TCGA(C/G) T(A/T)T(C/G)G(A/T)GTT-3') and KOD Dash polymerase (Toyobo). Other details were described in the literature (*25, 26*). These fragments were also subcloned into pGEM-T EASY Vector and sequenced. Based on the sequences of the cloned fragments, two primers (5'-AGCTGACCTTCGAGGCCTTCACGCT-3' and 5'-GACGAGTCCGCTGAACGGGAT -3') were synthesized and used to amplify the complete *hmd* gene from chromosomal DNA

with high fidelity KOD –plus– DNA polymerase (Toyobo) over 25 step-down cycles (*27*). The DNA fragments were purified from agarose gels and directly subjected to DNA sequence analysis in order to make sure of the final sequence (or exclude all PCR errors).

All DNA sequence analyses were performed by cycle sequencing techniques using a RISA-384 DNA sequencer. To confirm the DNA sequence of the entire gene and the expression construct pEThmd, DNA sequencing was performed on both strands using synthetic primers that were designed to bind at about 0.4 kbp intervals along the length of the gene. The *N. simplex hmd* sequence has been deposited in EMBL/GenBank/DDBJ under accession number AB120626. All oligonucleotides were purchased from Hokkaido System Science Co. The amino acid residues in alignment analysis are in HmDH numbering and the initiating methionine is assigned as residue 0 unless otherwise stated.

Expression and analysis of recombinant HmDH. For recombinant expression in *E. coli*, the *hmd* gene was amplified with KOD –plus– DNA polymerase using two primers (5'-catATGACCGAGCAGCCCGCCGT-3' and 5'-aagcttCAGAGTTGCGCCTCACGCCAG -3'; the residues printed in capital letters being complementary to the template sequence) from chromosomal DNA in the same manner as described above. The fragment was ligated into pGEM-T EASY Vector and sequenced. Then, this plasmid was digested with *Nde*I and *Hind*III (the *Nde*I and *Hind*III recognition sites being underlined in the sequences of the two primers) and inserted into pET-26b(+) (Novagen) to yield the expression construct pEThmd. The *E. coli* strain Rosetta(DE3) (Novagen) was transformed with pEThmd and grown in Luria-Bertani medium containing 0.1 % (W/V) glucose at 30 °C. In the late exponential phase, induction of recombinant protein expression was afforded by addition of isopropyl β-D-thiogalactoside (1 mM). Cells were harvested by centrifugation and disrupted by sonication in 0.01 M potassium phosphate buffer pH 7.5. Cell lysates were separated on SDS/PAGE and visualized by staining with Coomassie brilliant blue R250. HmDH activity in the soluble fraction of the cell lysates was assayed spectrophotometrically with phenazine methosulfate and 2,6-dichloroindophenol as described in the literature (*2*).

Isolation and analysis of the cofactor containing peptide. The cofactor-containing peptide was prepared as follows. HmDH was first reductively carboxymethyled; HmDH (1mg/ml) was reduced with 2 mg/ml of dithiothreitol for 5 h in 100 mM Tris-HCl buffer (pH 8.0) containing 6 M guanidine hydrochloride under Ar gas stream. The reduced sample was treated with a freshly prepared solution of iodoacetic acid (5 mg/ml) for 30 min. After concentration to about 10 mg/ml, the sample was digested for 24 h at 37 °C with lysyl endopeptidase (Wako) (0.4 mg/ml peptidase solution in 100 mM Tris-HCl pH 9.2). The cofactor-containing peptide was separated on a Symmetry 300 Å C_{18} column equilibrated with solvent A. The elution was in a linear gradient from 5 to 30 % of solvent B over 60 min and then a subsequent gradient to 60 % over 30 min at 40 °C. The cofactor-containing peptide fraction was lyophilized. The sample was dissolved in distilled water and 0.1 M potassium phosphate buffer pH 7.0 for Edman degradation analysis and UV-vis absorption spectroscopy, respectively. For ESMS analysis, however, the sample was dissolved in solvent C (0.2 % acetic acid, 50 % acetonitrile and 50 % H_2O) or solvent D (0.1 % trifluoroacetic acid, 50 % acetonitrile and 50 % H_2O).

Other Analytical Methods. Protein concentrations were determined based on both Biuret method (*28*) and modified Lowry method with a DC Protein Assay Kit (Bio-rad) using bovine serum albumin as a standard. Iron and acid-labile sulfur were determined by the published procedures (*29, 30*). UV-vis absorption spectra were recorded on a Shimadzu UV-2500PC spectrophotometer. EPR spectroscopy was performed as described in a previous paper (*9*).

RESULTS

Identification of hmd Gene Encoding Histamine dehydrogenase. N-terminal sequence analysis of the intact HmDH and of its internal peptide obtained by trypsin and chymotrypsin digestion revealed small regions of the sequence to be determined as N-terminal: TEQPAVAAPYDVLFEPVQIGPFTT*NRFY, and the internal peptide: IADPFLPNK (the amino acid residue indicated by asterisk could not be identified by Edman degradation

analysis). PCR with the corresponding degenerated primers yielded a 976 bp fragment. Based on the DNA sequence information on this fragment, two sets of three primers were synthesized for TAIL-PCR, which yielded two fragments of 355 bp and 763 bp in length. The sequence analysis revealed that the former fragment included the complete 5'-region of the *hmd* gene. However, the latter sequence obviously lacked the 3'-end of the *hmd* gene. The third try of TAIL-PCR was to use the other set of three primers, which resulted in the generation of about 2.5 kb amplicon including the missing part of the gene. Based on the sequence of the four PCR fragments, two primers were designed to amplify the complete *hmd* gene as one contiguous fragment. This amplification using high fidelity KOD –plus– DNA polymerase yielded a 2322 bp fragment. The independently amplified fragments were directly subjected to DNA sequence analysis at least three times. No conflict was observed on comparison of the resulting sequences, indicating the precise determination of the *hmd* gene sequence.

An open reading frame was identified in the fragment, which is 2073 bp in length and encodes a protein of 690 amino acids (including the N–terminal methionine residue which is absent when HmDH is expressed in *N. simplex*) (Fig. 2) with a calculated molecular weight of 75608 for an apoenzyme subunit, which is close to the reported values of the holoenzyme subunit about 84 kDa based on gel chromatographic and SDS/PAGE analyses (*2*). The *hmd* gene comprises 13.1 % T, 36.1 % C, 15.8 % A and 35.0 % G and has high GC contents as seen in many actinobacteria such as *Streptomyces* species. The analysis of the DNA sequence flanking the *hmd* gene failed to reveal sequence elements that would suggest the presence of promotor sequences. However, there is a putative stem-loop structure at the 3' end of the gene covering nucleotides 2097 to 2138: (5'-GCGCCCGGtACGGCGGCAGgggaCTGCCGCCG TgCCGGGCGC-3'; residues printed in capital letters corresponding to a putative stem-loop structure), which seems to act as a transcription termination signal. There is also a putative ribosome-binding site at the 5' end of the gene covering nucleotides from –10 to –13 (5'-AGGA-3'). The two-polypeptide sequences determined chemically are exactly identical with the corresponding portions of the deduced *hmd* amino acid sequence, respectively.

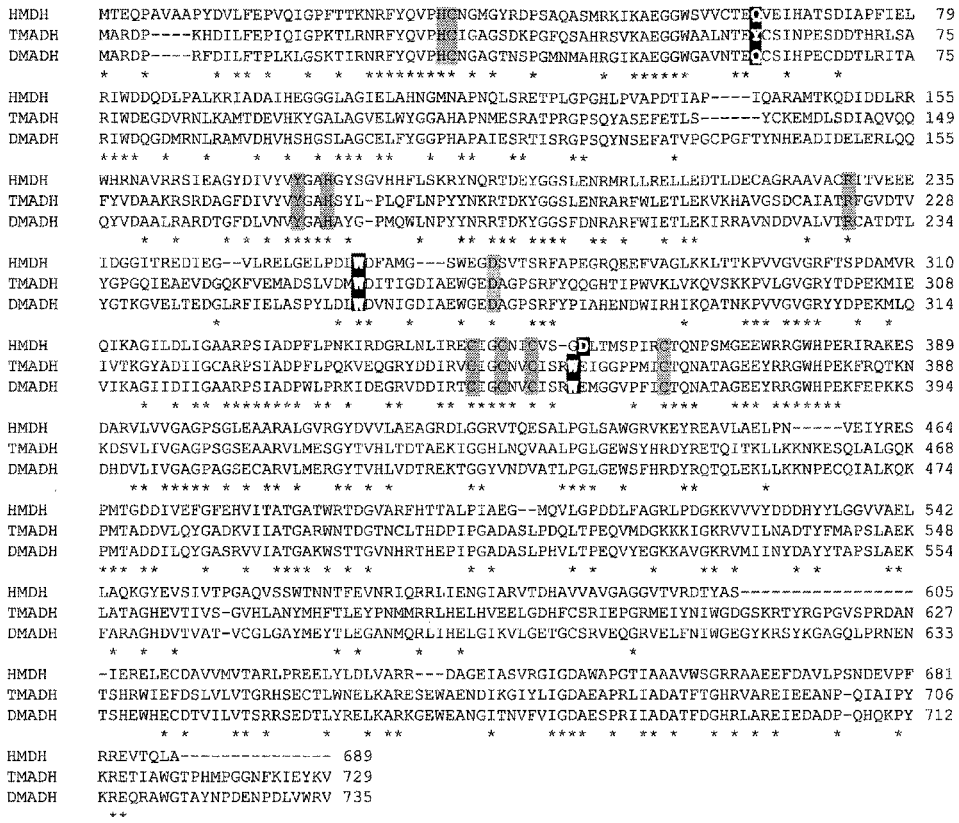

FIGURE 2: Sequence alignment of HmDH from *N. simplex* and related dehydrogenases. The present alignment was performed using the CLUSTAL W routine of the GenomeNet. All the amino-acid sequences of trimethylamine dehydrogenase from *M. methylotrophus* (W_3A_1) and dimethylamine dehydrogenase from *Hyphomicrobium X* were simultaneously compared with the histamine dehydrogenase sequence from *N. simplex*. The whole identities are 40.0 and 39.4 %, respectively and the sequences asterisked above are common residues. Residues that are shaded in gray are components of the active site and cysteines covalently linked to the cofactors, and those in black are the substrate-binding sites.

Recombinant expression of the wild type HmDH was achieved using bacterial expression vector pET-26b(+). The expression vector, designated pEThmd, brings the *hmd* gene under the control of the T7 promoter. Transformation of the vector into *E. coli* strain Rosetta (DE3) containing T7 RNA polymerase and induction with isopropyl β-D-thiogalactoside for 3 h resulted in the expression of a protein in a high yield with a molecular mass close to that of native HmDH (Fig. 3). The cell lysates exhibited strong HmDH activity. Without the induction treatment, however, *E. coli* strain Rosetta (DE3) with

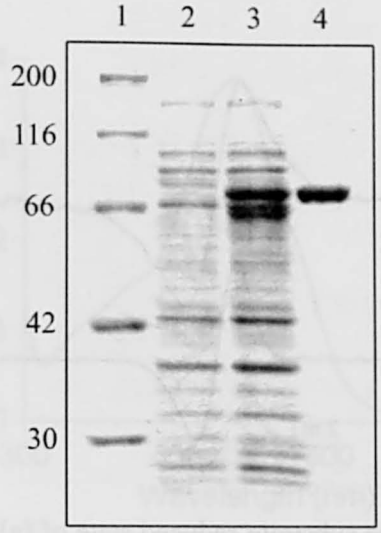

FIGURE 3: SDS/PAGE analysis of the expression of the *hmd* gene. Samples were separated by SDS/PAGE in a 10 % polyacrylamide gel and stained with Coomassie brilliant blue R250. Lane 1, molecular mass markers: myosin (200 kDa), β-galactosidase (116 kDa), bovine serum albumin (66.3 kDa), aldolase (42.4 kDa), carbonic anhydrase (30.0 kDa); lane 2, *E. coli* strain Rosetta (DE3) containing the pEThmd expression construct without induction; lane 3, *E. coli* strain Rosetta (DE3) containing the pEThmd expression construct after induction; lane 4, histamine dehydrogenase purified from *N. simplex*.

pEThmd didn't show any HmDH activity. These results indicate that the T7 promoter functions properly and that the *hmd* gene obtained in this study encodes HmDH exactly.

The Redox Active Prosthetic Groups of HmDH. It was suggested that HmDH would contain a covalently bound quinone-like organic cofactor, but details remained unknown (*2*). Comparisons of the deduced *hmd* amino acid sequence with the sequences deposited in the protein and DNA databases using the program FASTA revealed high similarity with TMADH from *Methylophilus methylotrophus* W_3A_1 and DMADH from *Hyphomicrobium X* (Fig. 2). TMADH and DMADH contain a covalently bound flavin coenzyme, 6-*S*-cysteinyl-FMN and also a tetrameric 4Fe-4S cluster as the redox active prosthetic groups (*14-17*). Alignment analysis of these two proteins with HmDH reveals that a 4Fe-4S cluster-binding motif is conserved in a portion of the amino acid residues from 346 to 355 including three cysteine residues (*31*). The forth cysteine for the cluster formation is also highly conserved as Cys365,

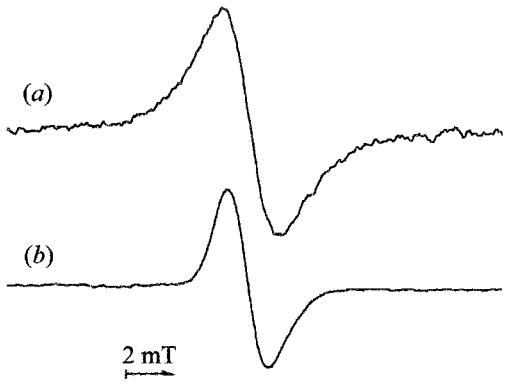

FIGURE 4: EPR spectra of the substrate-reduced state of (a) HmDH from *N. simplex* and (b) QH-AmDH from *P. denitrificans*. HmDH was reduced with excess amounts of histamine, while QH-AmDH was partially reduced with small amounts of *n*-butylamine in potassium phosphate buffer at pH 7.0 and at room temperature.

indicating that the HmDH subunit has one single iron-sulfur center [4Fe-4S]. Another cysteine residue to form covalent 6-*S*-cysteinyl-FMN is also conserved as Cys34 (*32*). Furthermore, two amino acid residues, His33 and Arg229, were conserved, which have been reported to play important roles in the post-translational formation of the cysteinyl bond as its reaction base (*33*) and as the stabilizer to neutralize negative charge on the N1/O2 atoms of the flavin (*34*), respectively (Fig. 1). These results suggest that HmDH has two redox active prosthetic groups as in the case of TMADH and DMADH.

Determination of the Two Redox Active Prosthetic Groups. HmDH prepared in high purity from *N. simplex* was analyzed on ESMS. Considering the experimental errors of the ESMS measurements, the multiply charged ion peaks were assigned to a protein with a molecular weight of $(75.9 \pm 0.1) \times 10^3$ (standard deviation from five determinations). The value is larger by ca. 0.4×10^3 than the apoenzyme subunit molecular weight (75477) calculated from the *hmd* sequence. The difference is in good agreement with the additional mass for 6-*S*-cysteinyl-FMN (molecular weight of FMN: 456) generated post-translationally. The 4Fe-4S iron-sulfur cluster must have been liberated from denaturated HmDH under the acidic conditions (pH $\cong$ 1) of the HPLC step.

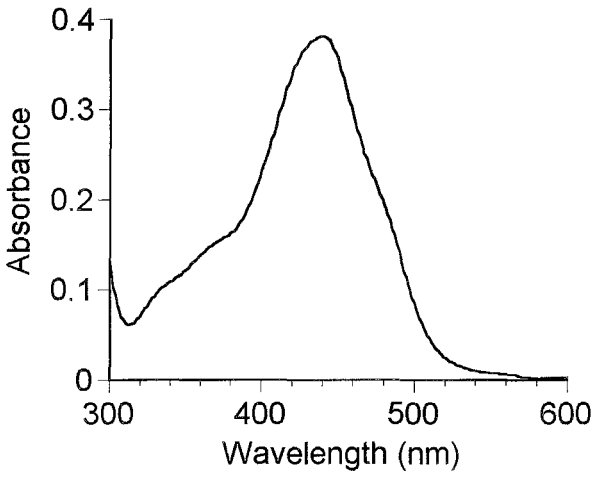

FIGURE 5: UV-vis absorption spectrum of the cofactor-containing peptide in HmDH. The absorption spectrum of the purified peptide was recorded in 0.1 M potassium phosphate buffer pH 7.0.

HmDH gave a strong EPR spectrum at $g \cong 2$ upon the reduction with excess amounts of histamine at pH 7.0 at room temperature (Fig. 4a), where a two-electron reduction of the enzyme must take place. The total line width of the EPR spectrum was ca. 6.0 mT, indicating the generation of a quinone-like organic radical. However, the line width was larger than that observed for CTQ-containing QH-AmDH from *P. denitrificans* (4.5 mT, Fig. 4b). This difference is interpretable by considering the coupling of the nitrogen atom(s) of 6-*S*-cysteinyl-FMN in HmDH. The EPR spectrum disappeared when HmDH was reduced with dithionite, indicating further reduction (most probably totally three-electron reduction) of HmDH. The generation of the flavo-semiquinone on substrate-reduction (two-electron reduction) suggests an intra-protein single electron transfer from the fully reduced flavin to a single-electron acceptor in HmDH.

In order to identify the covalently bound organic cofactor, HmDH was subjected to reductive carboxymethylation and subsequently digested with lysyl endopeptidase. The cofactor-containing peptide was purified by HPLC. The chromophore-containing peptide was eluted as a practically single peak. The absorption spectrum was very unique (Fig. 5). Automated Edman degradation of this peptide identified the following sequence: NRFYQVPH*NGMGYRDPSAQASMRK, which corresponds to the residues 26–50 in the

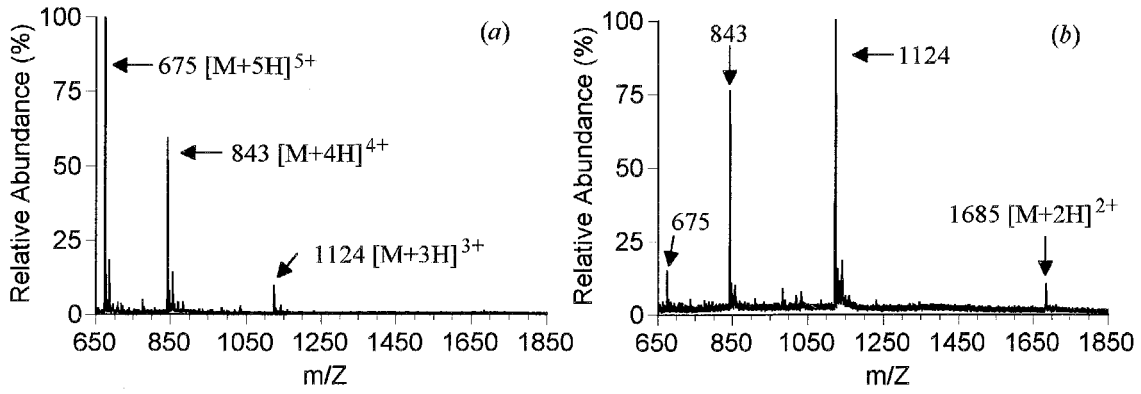

FIGURE 6: Positive mode ESMS spectrum of the cofactor-containing peptide in HmDH. The lyophilized sample was dissolved in solvent C (ca. 5 μM) containing 0.2 % acetic acid (a) and solvent D containing 0.1 % trifluoroacetic acid (b) just before ESMS analysis.

sequence of HmDH. The amino acid replaced with asterisk was not identified in Edman degradation analysis, and can be reasonably assigned to the site of the modified cysteine. This peptide was also subjected to ESMS analysis. When solvent C was used for the sample preparation (see experimental procedures), the three major multiply-charged ions were observed at *m/Z* of 675, 843 and 1124 (Fig. 6a). These peaks were assigned to $[M+5H]^{5+}$, $[M+4H]^{4+}$ and $[M+3H]^{3+}$, respectively. Another ion peak of *m/Z* 1685 to be assigned to $[M+2H]^{2+}$ was also observed when solvent D was used, although the total intensity of ion peaks decreased (Fig, 6b). The signals to be assigned to $[M+H]^{+}$ and $[M+6H]^{6+}$ could not be observed under the present conditions. As a result, the molecular weight of this peptide was determined by de-convolution to be 3368.6 ± 0.2 (standard deviation from eight determinations), which is identical with the value (3368.6) calculated for the corresponding sequence having 6-*S*-cysteinyl-FMN. These data verify that FMN is covalently bound to this peptide at Cys34.

Covalently linked forms of flavins occur more frequently in flavin adenine dinucleotide (FAD)-dependent enzymes than that in FMN-dependent ones. Covalently bound FAD is usually linked to histidine or cysteine residue at the 8α-methyl group of the isoalloxazine ring (*35*), and those absorption spectra are almost identical with those of non-covalent FADs (*36*). The peptide obtained in this experiment shows a spectrum with a

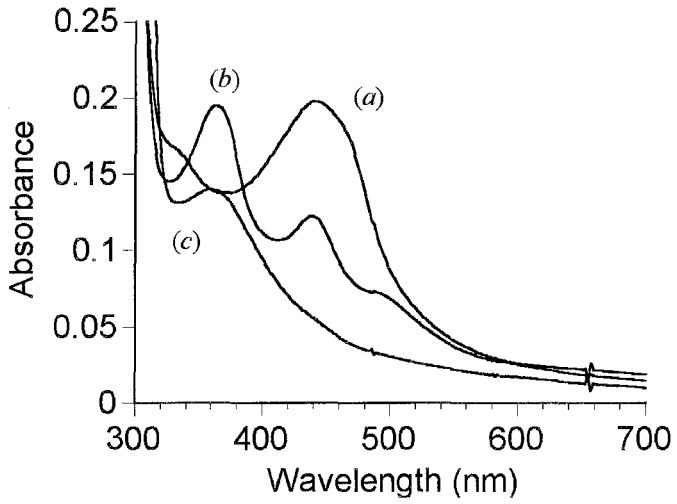

FIGURE 7: UV-vis absorption spectra of (a) the fully oxidized form, (b) substrate-reduced form, and (c) dithionite-reduced form of HmDH at pH 8.5. Substrate-reduced form was prepared by addition the substrate histamine to HmDH at a final concentration of 1 mM. Dithionite-reduced form was prepared by adding solid dithionite to the substrate reduced enzyme solution. A spectrum almost identical with (c) was obtained when HmDH was directly reduced with excess dithonite.

peak at 440 nm and a shoulder at 480 nm (Fig. 5), which is distinguished from that of FAD. The absorption spectrum has, rather, very close similarity with that of 6-*S*-cysteinyl-FMN in denaturated TMADH (*32*).

Another important point is to verify the presence of a ferredoxin-like 4Fe-4S cluster, which is included in TMADH and DMADH. Iron and acid-labile sulfur in HmDH were analyzed to be 7.6 moles and 8.1 moles per mole of HmDH, respectively. The absorption spectra of HmDH in the oxidized forms and substrate-reduced forms (Fig. 7 curves a and b) were almost identical with the corresponding spectra of TMADH and DMADH (*17, 37, 38*). The molar extinction coefficient of the fully oxidized HmDH was determined to be 48.3 mM^{-1} cm^{-1} at 442 nm on the basis of protein determination. This value is close to that of TMADH (52.3 mM^{-1} cm^{-1} at 443 nm) and DMADH (49.4 mM^{-1} cm^{-1} at 440 nm) (*39*). Addition of small amounts of solid dithionite to substrate-reduced HmDH (or the oxidized HmDH) caused further reduction of HmDH (Fig. 7 curve c), indicating the one-electron reduction of flavo-semiquinone. From these results, the author can safely conclude that HmDH has one covalently bound flavin, 6-S-cysteinyl-FMN, and one 4Fe-4S cluster as the redox active groups in each subunit.

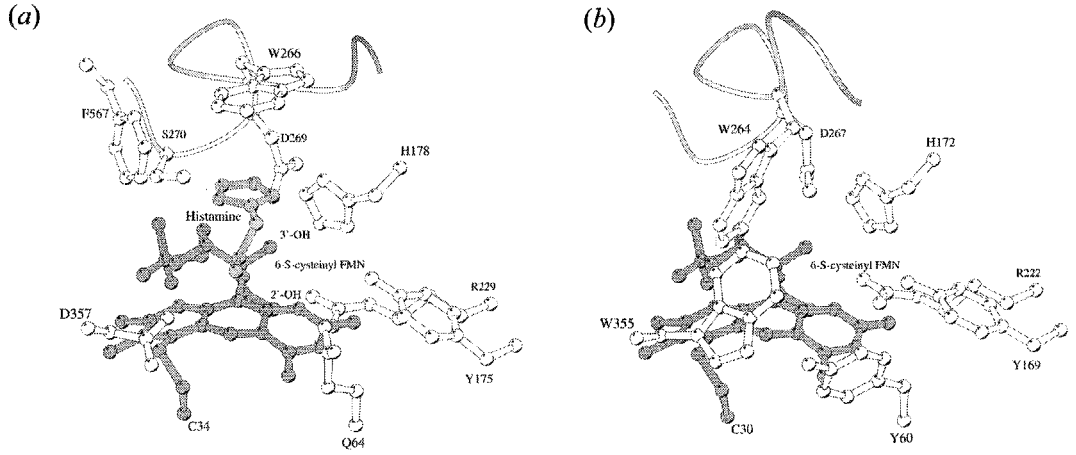

FIGURE 8: Catalytic centers of (a) histamine dehydrogenase model and (b) trimethylamine dehydrogenase. The coordinates used are those of the 2.4 Å structure of trimethylamine dehydrogenase. 6-*S*-Cysteinyl flavin mononucleotide is depicted in dark glay, histamine in light glay, and the amino acid residues in white. The graphics representation was generated using MOLSCRIPT software.

Preliminary Characterization of the Catalytic Center. Considering the high conservation in the sequence patterns among HmDH, TMADH, and DMADH, the overall structure and substrate-binding site are likely to be conserved among them. In this regard, the sequence alignment analysis may allow considering the residues that play significant catalytic roles. Actually, many residues in the active site are conserved, for example, Tyr175, His178, Arg229, Trp266 and Asp269 (*34, 40, 41*). For better understanding of the catalytic center of HmDH, homology modeling of the three-dimensional structure of HmDH was generated using the SWISS-MODEL server (http://www.expasy.org/swissmod/SWISS-MODEL.html) (*42*). The active site structure is shown in Fig. 8a, which was drawn with the program Molscript (*43*). In the theoretical model, the arrangement of the highly conserved residues, Tyr175, His178, Arg229 and Asp269, around the FMN is almost the same as that of TMADH. The hydroxyl group of Tyr175 forms a hydrogen bond with the imidazole side chain of His178. Arg229 and Asp269 are hydrogen bonded to ribityl 2'- and 3'- hydroxyl group of the FMN, respectively. On the other hand, Trp266 is also one of the highly conserved residues. However, a significant difference was suggested with respect to the orientation of its side-chain between

HmDH and TMADH. The indol ring of Trp266 is parallel to the *si*-face of flavin ring, whereas Trp264 in TMADH hangs over the middle portion of flavin with the approximately perpendicular orientation to each other (Fig. 8b). As shown in Fig. 2, the residues corresponding to 260-262 in TMADH are missing in HmDH. The loss of the three residues might result in the putative change that Trp266 is directed away from the flavin ring. In addition to the Trp residue described above, the residues corresponding to Tyr60 and Trp355 in TMADH, which are proposed to be involved in the substrate recognition (*21, 22*), are replaced with Gln64 and Asp357, respectively. Therefore, the substrate-binding cavity of HmDH appears to be quite different from that of TMADH in spite of the high sequence identity as a whole.

Furthermore, the author attempted to model the binding of substrate, histamine. The imidazole ring of histamine was positioned to occupy the space formed by the aromatic amino-acid residues: Trp266 and Phe567. Moreover, Ser270 was found inside the cavity. As a result, the protonated or deprotonated amino group of histamine was lying on the vicinity of the flavin N5. This is located suitably for catalysis: the α-hydrogen of the substrate would be transferred to the N5 of flavin (*41*).

DISCUSSION

HmDH resembles TMADH closely in various aspects such as the molecular weight, the subunit structure and amino acid sequence homology (40.0 % identical), suggesting homologous three-dimensional structure as a whole. The redox active centers involved in the catalysis and the subsequent electron transfer are identical with those of TMADH (and DMADH). HmDH is the third example of 6-*S*-cysteinyl-FMN- and Fe-4S cluster-containing enzymes. The HmDH reaction (Eq. (1)) seems to be somewhat different from those of TMADH and DMADH (Eq. (3)), but all the three enzymes catalyze oxidative N-C bond cleavage, and the reactions are very important in biological systems and essential in the nitrogen cycle on the earth.

Use of the program FASTA with EMBL/GenBank/DDBJ databases has suggested the occurrence of two TMADH-like proteins in *Sinorhizobium meliloti* and *Ralstonia*

solanacearum. However, these probable proteins are in higher homology with HmDH (*S. meliloti* (53.1 %) and *R. solanacearum* (51.5 %)) than with TMADH and DMADH. Actually, *S. meliloti* cultivated under suitable conditions showed HmDH activity (data not shown). Alignment analysis revealed that these probable proteins are very close to HmDH compared with TMADH and DMADH in view of similarities of amino acid sequence and several gap regions (data not shown). Details of the characterization of the corresponding enzyme from *S. meliloti* will be reported elsewhere in the future.

The oxidoreductases reactions can be divided into the oxidative half-reaction and the reductive half-reaction. The reductive half-reaction of HmDH involves oxidation of the substrate histamine: the two-electron transfer from the substrate to 6-*S*-cysteinyl-FMN in the enzyme active site and the subsequent N-C bond cleavage of the substrate. When HmDH was reduced by excess amounts of substrate, HmDH gave a strong EPR signal, which is assigned to the flavo-semiquinone radical (Fig. 4). The complete three-electron reduction of HmDH was achieved with excess amounts of dithionite, where the EPR spectrum disappeared. Corresponding phenomena were observed in UV-vis absorption spectroscopy (Fig. 7). Therefore, a single electron is transferred in the reductive half-reaction from dihydroflavin to the 4Fe-4S center to generate the flavo-semiquinone radical and the reduced iron-sulfur center. Similar phenomena have been reported for the reductive half-reaction of TMADH (*37, 38*). The EPR spectrum of the substrate-reduced enzyme was of particular interest, since it showed a complex pattern including a signal with $g \cong 4$ (referred to as the triplet state), indicative of the formation of a spin interacting state of the enzyme after generation of the flavo-semiquinone radical and the reduced iron-sulfur center (*37, 44-47*).

The oxidative half-reaction of HmDH should involve two single-electron transfer events from the reduced 4Fe-4S center to a two-electron acceptor or two single-electron acceptors, coupled with a single-electron transfer from the flavo-semiquinone to the 4Fe-4S cluster. Electron transferring flavoprotein (ETF) with FAD is believed to be the native single-electron acceptor of TMADH (*48*). The physiological electron acceptor of HmDH has not been identified yet. However, the physiological electron acceptor of HmDH seems to be different from ETF, because Tyr442 in TMADH, which is proposed to play a key role in the complex formation for the inter-protein electron transfer (*49, 50-52*), is not conserved.

Actually, any ETF-like protein could not be found in the purification process of HmDH in *N. simplex* in this study. Rather, production of a F420-like flavin derivative (*53*) was observed in *N.* simplex cells, but F420 did not work as an electron acceptor of HmDH (data not shown). Some single-electron acceptor such as cytochrome *c*, ferredoxin and azurin might be act as the native electron acceptor of HmDH.

A clear difference between HmDH and TMADH (or DMADH) is the substrate specificity. HmDH is active almost exclusively toward histamine, while low activity is observed for putrescine ($NH_2(CH_2)_4NH_2$) and agmatine ($NH_2(CH_2)_4NHC(NH)NH_2$) (*3*). Trimethylamine and dimethylamine cannot be oxidized at all (data not shown). In TMADH, it has been proposed that the natural substrate trimethylammonium cation binds to the enzyme through the interaction with the delocalized π electrons of three aromatic residues (Tyr60, Trp264 and Trp355) via cation-π bonding, which has recently been reported as unconventional ionic bonding (*54, 55*). The aromatic residues constitute a so-called "aromatic bowl". In DMADH, one of the three aromatic residues (Tyr60) in TMADH is replaced with glutamine (Gln60), and the other residues are conserved (*19*). Dimethylammonium cation may bind to the enzyme via hydrogen bonding between the N-H hydrogen atom of the substrate and the carbonyl group of Gln60 in addition to the cation-π bonding in the active site of DMADH (*22*).

It is noteworthy that the active site structure of HmDH appears to be quite different from that of TMADH. This situation would be responsible for the difference in the substrate selectivity. The putative active site space located at the *si*-face of the isoalloxazine ring (Fig. 8a) seems to be more suitable for compounds like histamine than bulky trimethylamine. In analogy with the above interaction schemes in TMADH and DMADH, it may be presumed that histamine may bind to HmDH via its protonated amino group as cation-π interaction. In this case, it appears, however, that the protonated amino group does not play a major role because HmDH has no activity toward various aliphatic and aromatic amines. In addition, the protonated amino group of histamine may be directing to Gln64 and Asp357, and the putative catalytic triad (Tyr175, His178 and Asp269) (*41, 47, 56*).

The three residues, Trp266, Phe567 and Ser270, might play an important role in the substrate recognition by stabilizing the imidazole moiety via the hydrogen bond formation

with the Ser270 hydroxyl group and π interaction with the aromatic amino acids as seen in several proteins (*1*). Considering, however, that putrescine and agmatine have protonated amino ($pK_a \cong 9$) and guanidino ($pK_a \cong 12$) group at optimum pH ≅ 8 of HmDH, respectively, these two amines may bind to the enzyme by the interaction with Trp266 and Phe567 via cation-π bonding in the same manner as has been proposed in choline binding site of acetylcholinesterase (*55*). Although pK_a of imidazole moiety of histamine is about 6.5, this group may be also protonated in the enzyme. The rational site-directed mutagenesis experiments based on sequence alignment study will be helpful for understanding the precise mechanism of the recognition of histamine. In addition, the author has recently succeeded in the crystallization of the wild type HmDH from *N. simplex* and the crystallographic analysis is on progress. The details may be reported elsewhere in the near future.

SUMMARY

Histamine dehydrogenase from *Nocardioides simplex* is a homodimeric enzyme and catalyzes oxidative deamination of histamine. The gene encoding this enzyme has been sequenced and cloned by polymerase chain reactions and over-expressed in *Escherichia coli*. The sequence of the complete open reading frame, 2073 bp coding for a protein of 690 amino acids, was determined on both strands. The amino acid sequence of histamine dehydrogenase is closely related to those of trimethylamine dehydrogenase and dimethylamine dehydrogenase containing an unusual covalently bound flavin mononucleotide, 6-*S*-cysteinyl-flavin mononucleotide, and one 4Fe-4S cluster as redox active cofactors in each subunit of the homodimer. The presence of the identical redox cofactors in histamine dehydrogenase has been confirmed by sequence alignment analysis, mass spectral analysis, UV-vis and EPR spectroscopy and chemical analysis of iron and acid-labile sulfur. These results suggest that the structure of histamine dehydrogenase in the vicinity of the two redox centers is almost identical to that of trimethylamine dehydrogenase as a whole. The structure modeling study, however, demonstrated that a putative substrate-binding cavity in histamine dehydrogenase is quite distinct from that of trimethylamine dehydrogenase.

REFERENCES

1. Konkimalla, V., B., and Chandra, N. (2003) *Biochem. Biophys. Res. Commun. 309*, 425–431.
2. Siddiqui, J. A., Shoeb, S. M., Takayama, S., Shimizu E., and Yorifuji, T. (2000) *FEMS Microbiol. Let. 189*,183–187.
3. Siddiqui, J. A., Shoeb, S. M., Takayama, S., Shimizu, E., Shimizu E., and Yorifuji, T. (2001) *J. Biochem. Mol. Biol. & Biophys. 5*, 37–43.
4. Husain, M., and Davidson, V. L. (1987) *J. Bacteriol. 169*, 1712–1717.
5. Iwaki, M., Yagi, T., Horiike, K., Saeki, Y., Ushijima, T., and Nozaki, M. (1983) *Arch. Biochem. Biophys. 220*, 253–262.
6. McIntire, W. S., Wemmer, D. E., Chistoserdov, A., and Lidstrom, M. E. (1991) *Science 252*, 817–824.
7. Govindaraj, S., Eisenstein, E., Jones, L. H., Sanders-Leohr, J., Chistoserdov, A. Y., Davidson, V. L., and Edwards, S. L. (1994) *J. Bacteriol. 176*, 2922–2929.
8. Shinagawa, E., Matsushita, K., Nakashima, K., Adachi, O., and Ameyama, M. (1988) *Agric. Biol. Chem. 52*, 2255–2263.
9. Takagi, K., Torimura, M., Kawaguchi, K., Kano, K., and Ikeda, T. (1999) *Biochemistry 38*, 6935–6942.
10. Datta, S., Mori, Y., Takagi, K., Kawaguchi, K., Chen, Z., Okajima, T., Kuroda, S., Ikeda, T., Kano, K., Tanizawa, K., and Mathews, F. S. (2001) *Proc. Natl. Acad. Sci. U.S.A. 98*, 14268–14273.
11. Satoh, A., Kim, J. K., Miyahara, I., Devreese, B., Vandenberghe, I., Hacisalihoglu, A., Okajima, T., Kuroda, S., Adachi, O., Duine, J. A., Van Beeumen, J., Tanizawa, K., and Hirotsu, K. (2002) *J. Biol. Chem. 277*, 2830–2834.
12. Steenkamp, D. J., and Mallinson, J. (1976) *Biochim. Biophys. Acta 429*, 705–719.
13. Meiberg, J. B. M., and Harder, W. (1979) *J. Gen. Microbiol. 115*, 49–58.
14. Hill, C. L., Steenkamp, D. J., Holm, R. H., and Singer, T. P. (1977) *Proc. Natl. Acad. Sci. USA 74*, 547–551.
15. Steenkamp, D. J., Kenney, W. C., and Singer, T. P. (1978) *J. Biol. Chem. 253*, 2812–2817.

16. Steenkamp, D. J., McIntire, W., and Kenney, W. C. (1978) *J. Biol. Chem. 253*, 2818–2824.

17. Steenkamp, D. J. (1979) *Biochem. Biophys. Res. Commun. 88*, 244–250.

18. Boyd, G., Mathews, F. S., Packman, L. C., and Scrutton, N. S. (1992) *FEBS Lett. 308*, 271–276.

19. Yang, C.-C., Packman, L. C., and Scrutton, N. S. (1995) *Eur. J. Biochem. 232*, 264–271.

20. Lim, L. W., Shamala, N., Mathews, F. S., Steenkamp, D. J., Hamlin, R., and Xuong, N. H. (1986) *J. Biol. Chem. 261*, 15140–15146.

21. Bellamy, H. D., Lim, L. W., Mathews, F. S., and Dunham, W. R. (1989) *J. Biol. Chem. 264*, 11887–11892.

22. Raine, A. R. C., Yang, C.-C., Packman, L. C. White, S. A., Mathews, F. S., and Scrutton, N. S. (1995) *Protein Sci. 4*, 2625–2628.

23. Basran, J., Mewies, M., Mathews, F. S., and Scrutton, N. S. (1997) *Biochemistry 36*, 1989–1998.

24. Inoue, H., Nojima, H., and Okayama, H. (1990) *Gene 96*, 23–28.

25. Liu, Y.-G. and Whittier, R. F. (1995) *Genomics 25*, 674–681.

26. Liu, Y.-G., Mitsukawa, N., Oosumi, T., and Whittier, R. F. (1995) *Plant J. 8*, 457–463.

27. Hecker, K. H., and Roux, K. H. (1996) *Biotechniques 20*, 478–485.

28. Itzhaki, R. F., and Gill, D. M. (1964) *Anal. Biochem. 9*, 401–410.

29. Massey, V. (1957) *J. Biol. Chem. 229*, 763–770.

30. Chen, J.-S., and Mortenson, L. E. (1977) *Anal. Biochem. 79*, 157–165.

31. Barber, M. J., Neame, P. J., Lim, L. W., White, S., and Matthews, F. S. (1992) *J. Biol. Chem. 267*, 6611–6619.

32. Scrutton, N. S., Packman, L. C., Mathews, F. S., Rohlfs, R. J., and Hille, R. (1994) *J. Biol. Chem. 269*, 13942–13950.

33. Packman, L. C., Mewies, M., and Scrutton, N. S. (1995) *J. Biol. Chem. 270*, 13186–13191.

34. Mewies, M., Packman, L. C., Mathews, F. S., and Scrutton, N. S. (1996) *Biochem. J. 317*, 267–272.

35. Mewies, M., McIntire, W. S., and Scrutton, N. S. (1998) *Protein Sci. 7*, 7–20.

36. Edmondson, D. E., and Singer, T. P. (1973) *J. Biol. Chem. 248*, 8144–8149.

37. Steenkamp, D. J., and Singer, T. P. (1978) *Biochem. J. 169*, 361–369.

38. Steenkamp, D. J., and Beinert, H. (1982) *Biochem. J. 207*, 233–239.

39. Kasprzak, A. A., Papas, E. J., and Steenkamp, D. J. (1983) *Biochem. J. 211*, 535–541.

40. Basran, J., Jang, M. H., Sutcliffe, M. J., Hille, R., and Scrutton, N. S. (1999) *J. Biol. Chem. 274*, 13155–13161.

41. Basran, J., Sutcliffe, M. J., and Scrutton, N. S. (2001) *J. Biol. Chem. 276*, 42887–42892.

42. Guex, N., and Peitsch, M. C. (1997) *Electrophoresis 18*, 2714–2723.

43. Kraulis, P. J. (1991) *J. Appl. Crystallogr. 26*, 283–291.

44. Steenkamp, D. J., and Beinert, H. (1982) *Biochem. J. 207*, 241–245.

45. Stevenson, R. C., Dunham, W. R., Sands, R. H., Singer, T. P., and Beinert, H. (1986) *Biochim. Biophys. Acta 869*, 81–88.

46. Fournel, A., Gambarelli, S., Guigliarelli, B., More, C. Asso, M., Chouteau, G., Hille, R., and Bertrand, P. (1998) *J. Chem. Phys.109*, 10905–10913.

47. Jang, M. H., Basran, J., Scrutton, N. S., and Hille, R. (1999) *J. Biol. Chem. 274*, 13147–13154.

48. Steenkamp, D. J., and Gallup, M. (1978) *J. Biol. Chem. 253*, 4086–4089.

49. Wilson, E. K., Mathews, F. S., Packman, L. C., and Scrutton, N. S. (1995) *Biochemistry 34*, 2584–25891.

50. Wilson, E. K., Huang, L., Sutcliffe, M. J., Mathews, F. S., Hille, R., and Scrutton, N. S. (1997) *Biochemistry 36*, 41–48.

51. Basran, J., Chohan, K. K., Sutcliffe, M. J., and Scrutton, N. S. (2000) *Biochemistry 39*, 9188–9200.

52. Leys, D., Basran, J., Talfournier, F., Sutcliffe, M. J., and Scrutton, N. S. (2003) *Nat. Struc. Biol. 10*, 219–225.

53. Ebert, S., Rieger, P.-G., and Knackmuss, H.-J. (1999) *J. Bacteriol. 181*, 2669–2674.

54. Deakyne, C. A., and Meot-Ner, M. (1985) *J. Am. Chem. Soc. 107*, 474–479.

55. Scrutton, N. S., and Raine, A. R.C. (1996) *Biochem. J. 319*, 1–8.

56. Basran, J., Sutcliffe, M. J., Hille, R., and Scrutton, N. S. (1999) *Biochem. J. 341*, 307–314.

2.2. Production of Completely Flavinylated Histamine Dehydrogenase, Unique Covalently Bound Flavin, and Iron-Sulfur Cluster-Containing Enzyme of Nocardioides simplex in Escherichia coli, and Its Properties

Histamine is produced in improperly handled foods as a result of the bacterial decarboxylation of histidine, and is used as a marker for unsafe foods. The development of detection methods for histamine is one of the major interests in food chemistry. Recently, histamine dehydrogenase (HmDH) was discovered in *Nocardioides simplex*, one of the Gram-positive actinobacteria (*1,2*). The enzyme is a homodimer and catalyzes the oxidative deamination of histamine to imidazole acetaldehyde and ammonia. It was preliminary classified by quinone staining and UV-vis spectroscopy into the quinoprotein family (*1*), which includes methylamine dehydrogenase (*3*) and quinohemoprotein amine dehydrogenase (*4,5*). But on the basis of molecular cloning and mass spectrometry, it has been reassigned to the iron-sulfur cluster flavoprotein family (*6*), and in particular is related to trimethylamine dehydrogenase (TMADH) (*7*) and dimethylamine dehydrogenase (*8*), and contains [4Fe-4S] cluster and an unusual covalently bound flavin, 6-*S*-cysteinyl-FMN (*9,10*).

The enzyme shows unique and narrow substrate specificity and thermal stability, and does not use molecular oxygen as an electron acceptor (*1,11*). These properties provide several advantages for utilization in histamine sensors (*12*). In addition, it is very interesting to investigate the mechanism of the enzymatic recognition to histamine. Hence, there is a large demand for overproduction of the recombinant enzyme for related research in biosensors and biochemistry. Several flavoproteins with covalently bound flavin, however, have been produced with apoprotein in heterologous hosts (*13,14*). Especially, the recombinant TMADH produced in *E. coli* strain JM109 was not fully flavinylated (about 25% of flavinylation) (*15*). In our previous study, the *hmd* gene was overexpressed in *E. coli* strain Rosetta (DE3) using a pET26b(+) vector (*6*). In the present study, the author purified the recombinant enzyme to homogeneity and verified complete flavinylation.

EXPERIMENTAL PROCEDURES

E. coli strain Rosetta (DE3) (Novagen) transformed with expression construct

pEThmd (*6*), in which the *hmd* gene was subcloned under the control of the T7 promoter of pET26b(+) without the addition of any peptide-tags, was grown on Luria-Bertani medium supplemented with 0.1% (W/V) glucose, 20 mg/l kanamycin, 34 mg/l chloramphenicol, 50mg/l riboflavin, and 200 mg/l $FeSO_4$ at 30°C. Induction of *hmd* gene expression was afforded by the addition of isopropyl β-D-thiogalactoside (1 mM) 5 h after the late exponential phase (OD ≅ 1.0).

Recombinant HmDH was purified as follows: The cells were disrupted in a French press at a cell pressure of 140 Mpa in buffer A (0.01 M potassium phosphate buffer, pH 7.5). Cell debris and the insoluble fraction were removed by centrifugation (12,000 × *g* for 30 min), and the supernatant was clarified by ultracentrifugation (180,000 × *g* for 90 min). The supernatant was then charged on a DEAE–Sepharose column (r = 5 cm, l = 20 cm) (Amersham), equilibrated with buffer A, and eluted with a linear gradient (800 ml) of buffer A containing 0.3–0.6 M NaCl. The fractions (80 ml) were pooled and dialyzed against two changes of buffer A containing 0.8 M $(NH_4)_2SO_4$ (4-liter each). The dialyzed enzyme was applied to a Butyl-Toyopearl 650 M column (r = 2.5 cm, l = 15 cm) (Tosoh). The column was washed and eluted using a decreasing linear gradient (600 ml) of $(NH_4)_2SO_4$ from 0.8 M to 0.25 M. The fractions (70 ml) were collected and dialyzed two times against buffer A. The protein was then loaded onto a DEAE-Toyopearl 650 M column (r = 2.5 cm, l = 15 cm) (Tosoh) and eluted using a linear gradient increasing from 0.15 M to 0.4 M NaCl (buffer A). The enzyme fraction was then injected to a column of Hiload 26/60 Superdex 200 pg (Amersham) equilibrated with 0.05 M sodium phosphate, pH 7.5, containing 0.15 M NaCl. Finally, the enzyme was purified with a Ceramic Hydroxyapatite Type I (Bio-Rad) eluted with a linear gradient of 10–200 mM potassium phosphate buffer of pH 6.8.

RESULTS AND DISCUSSION

The recombinant enzyme was highly purified, and appeared to have the same molecular weight and subunit structure as those of the native enzyme from *N. simplex*, as judged by SDS-PAGE and Native-PAGE (Fig. 1A and B). The yield of pure protein was typically in the range from 6 to 10 mg/l culture. The values indicate sufficiently high yield as

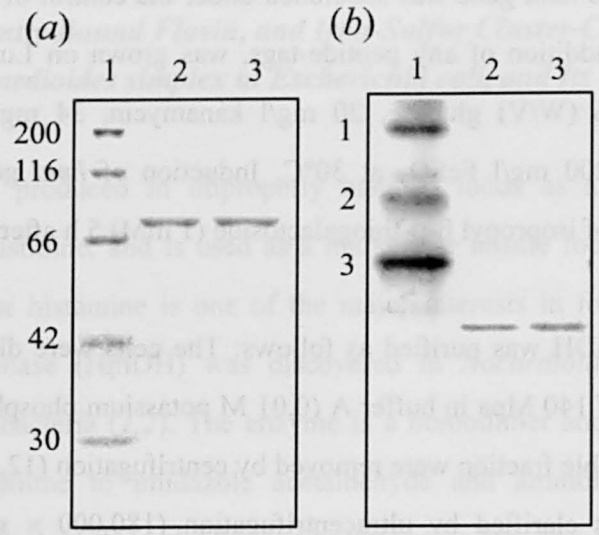

FIGURE 1. PAGE Analysis of HmDH. Panel *a*, SDS-PAGE with a 12.5% polyacrylamide gel. Lane 1, molecular mass markers: myosin (200 kDa), β-galactosidase (116 kDa), bovine serum albumin (66.3 kDa), aldolase (42.4 kDa), carbonic anhydrase (30.0 kDa); lane 2, native histamine dehydrogenase purified from *E. coli* (1 μg); lane 3, recombinant histamine dehydrogenase purified from *N. simplex* (1 μg). Panel *b*, Native-PAGE with a 10% polyacrylamide gel. Lane 1, markers: band 1, human hemoglobin A (64.5 kDa); band 2, phycocyanin (232 kDa); band 3, equine myoglobin (17.5 kDa); lane 2, native histamine dehydrogenase purified from *E. coli* (1 μg); lane 3, recombinant histamine dehydrogenase purified from *N. simplex* (1 μg). The proteins were stained with Coomassie brilliant blue R250.

compared to that of pure native enzyme (≅ 0.5 mg/l culture) (*1*). The first five residues of the N-terminal amino acid sequence were found to be Met-Thr-Glu-Asn-Pro for the major peak, although a minor peak with an N-terminal sequence of Thr-Glu-Asn-Pro-Ala was also observed. The sequence of the major peak exactly matched those predicted from the DNA sequence of the *hmd* gene (Met-Thr-Glu-Asn-Pro) (*6*), while that of the minor peak was identical with that the native enzyme (Thr-Glu-Asn-Pro-Ala) (*6*). This means that most of the recombinant enzymes retain the amino-terminal methionine residue, which is lacking in the native one. The specific activities of the native and recombinant enzyme were determined to be 45 and 43 $\mu mol \cdot min^{-1} \cdot mg^{-1}$ respectively by measuring the amine-dependent reduction rate of the ferricenium ion at 617 nm. The assays were performed in 0.1 M potassium phosphate

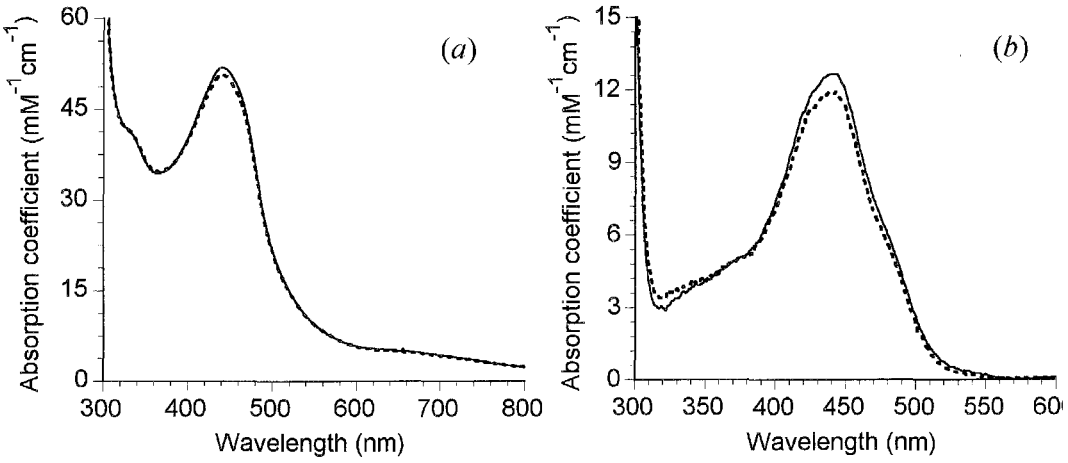

FIGURE 2. UV-Vis Spectra of Histamine Dehydrogenase and Acid-Treated Histamine Dehydrogenase. Panel *a*, UV-vis spectra of native (solid line) and recombinant enzyme (broken line). Panel *b*, UV-vis spectra of perchloric acid-treated (solid line) native and (broken line) recombinant HmDH. The enzymes were precipitated with 0.5 M perchloric acid and re-solubilized with 6 M guanidine hydrochloride in 0.1 M potassium phosphate buffer, pH 7.5. The millimolar absorption coefficient is referred to a single enzyme subunit.

buffer, pH 7.5, containing 1 mM histamine and 350 μM ferricenium hexafluorophosphate at 30°C.

The visible absorption spectrum of the fully oxidized form of the recombinant enzyme exhibited a peak centered at 441 nm and a shoulder at 340 nm, and was almost identical with that of the native enzyme, described in our previous paper (*6*) (Fig. 2a). The molar absorption coefficients of the fully oxidized native and recombinant enzymes were determined to be 51.9 ± 2 and 50.0 ± 3 $mM^{-1}\,cm^{-1}$ respectively at 441nm, on the basis of protein determination by amino acid analysis. Judging from the spectra, it was expected that the recombinant enzyme would have two redox cofactors identical to those of the native enzyme, a [4Fe-4S] cluster and a covalently bound flavin, 6-*S*-cysteinyl-FMN.

Quantitative analysis of the cofactors in the recombinant enzyme was performed to verify complete incorporation of the cofactors in the recombinant enzyme. Iron and acid-labile sulfur in the recombinant enzyme were analyzed to be 7.4 moles and 8.2 moles per mole of enzyme respectively, by published procedures (*16, 17*). This demonstrates that the enzyme has

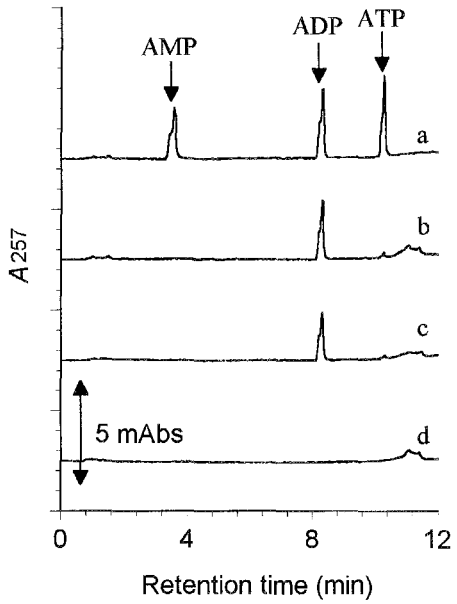

FIGURE 3. Chromatograms of (a) a Standard Nucleotide Mixture (each 0.13nmol), Nucleotide Bound to (b) Native HmDH (0.1 nmol) and (c) Recombinant HmDH (0.09 nmol) on Ion-Pair Reverse Phase HPLC. Curve d is a background chromatogram. Elution was performed with a linear gradient from buffer B (50 mM sodium phosphate buffer containing 10 mM tetrabutylammonium, pH 6.6) to 40 % (V/V) methanol in 10 min at a flow rate of 1.5 ml/min at 40°C. Elution of nucleotides was monitored at 257 nm with a diode array unit.

one [4Fe-4S] cluster per subunit. On the other hand, the binding state and contents of the flavin cofactor were studied spectrophotometrically for the recombinant enzyme as well as the native enzyme. The recombinant and native enzymes were precipitated with 0.5 M perchloric acid. The supernatant after centrifugation gave no absorption band derived from non-covalently bound flavin. The acid-precipitated enzyme samples that lost the ion-sulfur cluster were re-solubilized with 6 M guanidine hydrochloride solution in 0.1 M potassium phosphate, pH 7.5. The denaturated enzyme solutions showed a unique absorption spectrum (Fig. 2b) closly similar to that of the peptide containing 6-*S*-cysteinyl-FMN derived from the native enzyme (*6, 13*). These results clearly confirm that 6-*S*-cysteinyl-FMN is suitably formed in the recombinant enzyme. The absorbance at 440 nm was proportional to the protein concentration (determined by amino acid analysis). Assuming that the native enzyme is fully flavinylated (100 %), the flavinylation ratio of the recombinant enzyme can be calculated to

be 93%. It can safely be concluded that 6-*S*-cysteinyl-FMN is almost completely assembled in the recombinant enzyme.

As previously reported, TMADH contains one molecule of ADP per subunit, although its function remains unknown. This ADP binding domain is conserved in HmDH, and aligns with the FAD binding region of other proteins (*11*). In order to confirm the occurrence of ADP, nucleotide analysis was undertaken as follows: The three nucleotides, AMP, ADP and ATP, were completely separated by ion-pair reverse phase chromatography using a TSKgel Super-ODS column (4.6 × 100mm, Tosoh) and a tetrabutylamine ion-pair/methanol gradient (18) (Fig. 3, a). A nucleotide sample was prepared by precipitating the protein with 5% trichloroacetic acid, followed by centrifugation. The supernatant containing nucleotides was diluted 5-fold with buffer B and then injected into ion-paired reversed phase HPLC without further purification. The samples of native and recombinant enzyme gave one sharp peak in HPLC analysis under the present conditions (Fig. 3, b and c). The retention time of the peak due to the putative nucleotide derived from the native and recombinant proteins was identical with that of a standard ADP solution, indicating that the enzymes contained ADP. In order to quantify the amount of ADP bound to the enzyme, the enzyme was precipitated with 0.5 M perchloric acid, and the protein was removed by centrifugation. The concentration of the released ADP in the supernatant was quantified by absorption spectroscopy. ADP in the native and recombinant enzyme was analyzed to be 1.7 moles and 1.8 moles per mole of the enzyme respectively, indicating that the enzyme had one ADP per subunit.

These results suggest that the recombinant enzyme is practically identical with the native enzyme. In contrast with TMADH, the purified recombinant HmDH is completely flavinylated. It appears that the flavinylation on Cys35 at C6 of the isoalloxazine ring of FMN proceeded auto-catalytically in recombinant HmDH. Production of apoprotein cannot be ruled out in the present case, but holoprotein was almost completely separated from apoprotein, if any, by the proposed purification method, as in the case of recombinant dimethylglycine dehydrogenase (*14*). The recombinant HmDH can safely be used as a substitute for the native enzyme, and this preparation method for recombinant HmDH should open a route for utilization of the enzyme for histamine biosensors and should also make it easy to study various mechanisms of the enzyme in combination with the utilization of site-directed

mutagenesis, for example, electron transfer reaction and substrate recognition.

SUMMARY

The *hmd* gene of histamine dehydrogenase from *Nocardioides simplex* was overexpressed in *Escherichia coli*, and the resulting enzyme was purified to homogeneity. The purified recombinant enzyme is almost identical with the native enzyme in view of molecular weight and specific activity, and is stoichiometrically assembled with the three cofactors 6-*S*-cysteinyl-FMN, 4Fe-4S cluster, and ADP.

REFERENCES

1. Siddiqui, J.A., Shoeb, S.M., Takayama, S., Shimizu, E., and Yorifuji, T. (2000) *FEMS Microbiol.* Lett. *189*, 183–187.
2. Siddiqui, J.A., Shoeb, S.M., Takayama, S., Shimizu, E., and Yorifuji, T., (2001) *J. Biochem. Mol. Biol. Biophys. 5*, 37–43.
3. McIntire, W.S., Wemmer, D.E., Chistoserdov, A., and Lidstrom, M.E., (1991) *Science, 252*, 817–824.
4. Datta, S., Mori, Y., Takagi, K., Kawaguchi, K., Chen, Z., Okajima, T., Kuroda, S., Ikeda, T., Kano, K., Tanizawa, K., and Mathews, F.S. (2001) *Proc. Natl. Acad. Sci. U.S.A. 98*, 14268–14273.
5. Satoh, A., Kim, J.K., Miyahara, I., Devreese, B., Vandenberghe, I., Hacisalihoglu, A., Okajima, T., Kuroda, S., Adachi, O., Duine, J. A., Van Beeumen, J., Tanizawa, K., and Hirotsu, K. (2002) *J. Biol. Chem., 277*, 2830–2834.
6. Fujieda, N., Satoh, A., Tsuse, N., Kano, K., and Ikeda, T. (2004) *Biochemistry, 43*, 10800–10808.
7. Steenkamp, D.J., and Mallinson, J. (1976) *Biochim. Biophys. Acta 429*, 705–719.
8. Meiberg, J.B.M., and Harder, W. (1979) *J. Gen. Microbiol. 115*, 49–58.
9. Steenkamp, D.J., Kenney, W.C., and Singer, T.P. (1978) *J. Biol. Chem. 253*, 2812–2817.
10. Steenkamp, D.J., McIntire, W.S., and Kenney, W.C., (1978) *J. Biol. Chem., 253*,

2818–2824.

11. Limburg, J., Mure, M., and Klinman, J.P. (2005) *Archives Biochem. Biophys. 436*, 8–22.
12. Takagi, K., and Shikata, S. (2004) *Anal. Chim. Acta, 505*, 189–193.
13. Hederstedt, L., Bergman, T., and Jijrnvall, H. (1987) *FEBS Lett. 213*, 385–390.
14. Brizio, C., Brandsch, R., Bufano, D., Pochini, L., Indiveri, C., and Barilea, M., (2004) *Protein Expr. Purif. 37*, 434–442.
15. Scrutton, N.S., Packman, L.C., Mathews, F.S., Rohlfs, R.J., and Hille, R., (1994) *J. Biol. Chem. 269*, 13942–13950.
16. Vanoni, M.A., Edmondson, D.E., Zanetti, G., and Curti, B. (1992) *Biochemistry 31*, 4613–4623.
17. Chen, J.-S., and Mortenson, L.E. (1977) *Anal. Biochem. 79*, 157–165.
18. Techel, D., and Braumann, T., (1989) *J. Chromatogr. 483*, 427–430.

2.3. Bioelectrocatalytic Detection of Histamine with Histamine Dehydrogenase-Based Electrode

Biogenic amines are useful as possible biomarkers for food quality and control. Histamine is one of the most known compounds of this class and can be found in improperly handled foods, especially fish or fish products, as a result of the bacterial decarboxylation of histidine and may be accumulated to toxic levels. Thus, histamine concentration is a good indicator of food freshness and analysis of histamine is the major concerns in food chemistry. For the determination of histamine, the currently recommended procedure is based on chromatographic techniques, which require fluorescence derivatization and expensive instrumentation (*1-3*). Amperometric biosensors based on suitable enzymes coupled with artificial electron acceptors have also been developed using histamine oxidase (*4, 5*), methylamine dehydrogenase (*6-8*), and quinohemoprotein amine dehydrogenase (*9*). However, these methods have some disadvantages in substrate specificity or interference from molecular oxygen.

Recently, histamine dehydrogenases (HmDH) have been discovered from *Nocardioides simplex*, one of Gram-positive actinobacteria (*10*) and *Rhizobium* species (11). These enzymes catalyze the oxidative deamination of histamine to imidazole acetaldehyde and ammonia. The enzyme shows its highest activity toward histamine among various amines. In addition, the enzyme is thermally stable, and does not use molecular oxygen as an electron acceptor. (*10-12*). These properties would provide several advantages for utilization in histamine sensors. By using this enzyme-based electrode, a flow injection analysis system for the determination of histamine was developed (*13*). However, the methods were operating at high potential of +0.4 V vs. SHE, which increases interference from electro-active substances such as ascorbate. In this study, the author investigated the possibility to amperometric detection of histamine at a low applied potential, using HmDH and osmium-derivative polymer (PVI-dpaOs).

EXPERIMENTAL PROCEDURES

Materials. Histamine dihydrochloride was purchased from Sigma-Aldrich Co. PVI-dpaOs was prepared as described in the literature (*14*). Poly(ethylene glycol) diglycidyl ether (PEGDGE, Aldrich) was used for crosslinking the enzyme to the Os modified polymer. All other chemicals were reagent grade and were used without further purification. Recombinant HmDH was prepared and purified as described previously (*15*).

Electrode preparation. Glassy carbon electrode was polished with 0.05 μm alumina powder and sonicated in deionized water for about 5 min. Three microliters of an enzyme stock solution (10 mg ml/1), 6 μl of PVI-dpaOs (5 mg ml/1 in water), and 3 μl of crosslinker PEGDGE (3 mg ml/1 in water) were mixed, and 3 μl of the mixture was pipetted onto a GC electrode (i.d. 3.0 mm) (Bioanalytical Systems). The electrode was cured for 16 h at 37 °C before use.

Electrochemical measurements. Cyclic voltammetry was performed with a BAS 50W potentiostat (Bioanalytical Systems) using an Ag/AgCl/KCl (sat.) reference electrode and a Pt-disk counter electrode. The electrochemical measurements were performed under anaerobic conditions at 30 °C in 100 mM potassium phosphate buffer (pH 7.0) adjusted to I_s = 0.3 with KCl. Constant potential amperometric determination of histamine was done at +0.2 V under stirring. All redox potentials in this paper are referred to the standard hydrogen electrode (SHE) unless otherwise stated.

RESULTS AND DISSCUSION

As shown by the broken line in Fig. 1, the stationary cyclic voltammogram obtained at the HmDH/Os-modified GC electrode showed a pair of redox waves around +0.1 V, assigned to the redox reaction of $Os^{2+/3+}$. The peak separation of about 80 mV (v = 10 mVs^{-1}) between the cathodic and anodic waves was larger than that as described previously (*14*), probably because the scan rate was faster than that in the previous study. In the presence of an excess

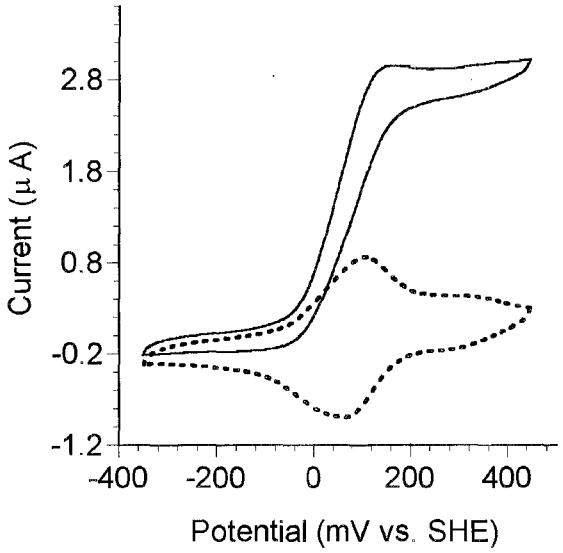

FIGURE 1: Cyclic voltammograms of a HmDH/Os-modified GC electrode in the absence (broken line) and presence (solid line) of 5 mM histamine at a scan rate of 10 mV s^{-1}.

amount of histamine, the voltammogram developed typical catalytic characteristics (Figure 1, solid line). Such a catalytic wave was not observed at the Os-modifed electrode without HmDH. This indicated that HmDH was successfully immobilized on the polymer, and the Os redox polymer acted as an efficient electron-transfer mediator between HmDH and the electrode. The wave of the sigmoidal-shape reached a plateau at +0.2 V; namely, the reaction between Os redox polymer and GC electrode is very fast at potential of ≥ +0.2 V under this condition.

At a fixed electrode potential of +0.2 V, the catalytic currents increased on the addition of histamine, indicating response to histamine. Figure 2a shows an example of the amperometric response for the successive injections of histamine under stirring. Fig. 2b shows the calibration curves obtained with the HmDH/Os-modified electrode. The plot of the current against the concentration of histamine satisfied a linear relationship over the range from 2 to 50 μM. The upper limit of the linearity is as small as the Michaelis constant (K_s) of HmDH for histamine (0.075 mM) (*10*). From this result, it appears that the rate-determining step could not be the permeation process of histamine across the immobilized membrane but enzyme kinetics in this sensor. However, response time, especially that for the first injection of

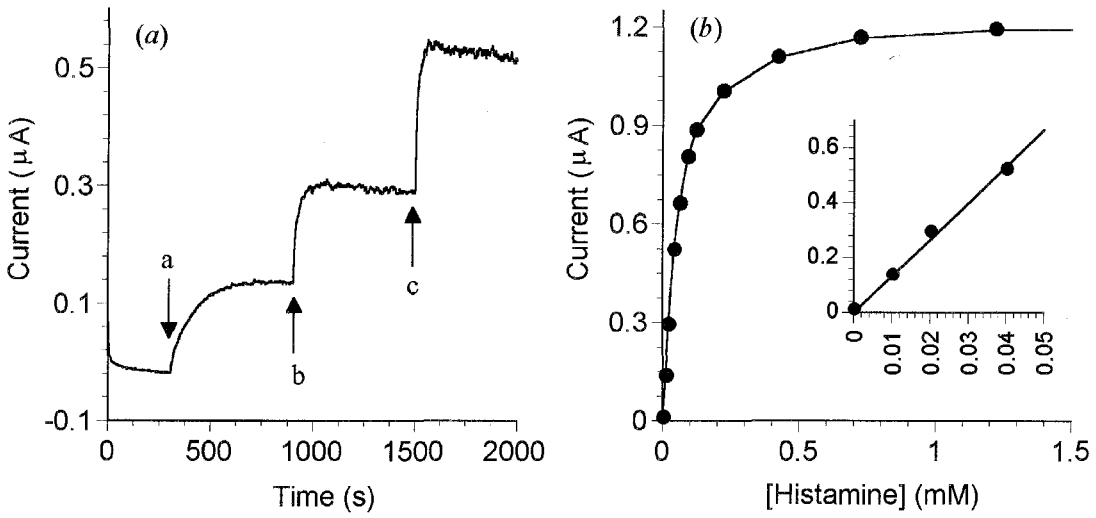

FIGURE 2: Amperometric response of a HmDH/Os-modified GC electrode at a fixed applied potential of + 0.2 V. (*a*) Current–time curves. Histamine was added, in turn, to the solution at arrows a, b, and c to make 10 μM, 20 μM and 40 μM each. (*b*) Calibration curves of histamine.

histamine, is relatively large (about 1 min for 90 %-gain). Interestingly, the response current showed hyperbolic dependence on histamine concentration like Michaelis-Menten curve, although this enzyme clearly showed substrate inhibition at ≥ ca. 100 μM histamine under soluble condition (Data not shown). These results might suggest that the catalytic activity of the immobilized HmDH was different from that of native one, or the condition in the immobilized membrane, such as pH and ionic strength, depended on the concentration of histamine.

Maximum permissible limits for histamine in foods, which prescribed in Europe, are ca. 150 mg/kg in fish and fish products and ca. 50mg/kg in wine. It is noted that the linearity of this HmDH/Os-modified electrode would cover the histamine level in food and achieved acceptable performance to cover the concentration range at a working potential of +0.2 V. The utilization of PVI-dpaOs allowed the author to detect histamine electrochemically at a low potential of +0.2 V. However, several points remain to be improved. The HmDH-based electrode using PVI complexed with [osmium (4,4'-dimehylbipyridine)$_2$Cl] polymer as electron mediators was characterized previously (*13*). The electrode didn't response to other primary amines, but to ascorbate, a common component of blood and biological samples. In

this work, HmDH/Os-modified electrode also responded to ascorbate at relatively low magnitude, although other electroactive substances such as urate did not interfere the response. Thus, the interference of ascorbate is one of the most serious problems to overcome; however, some attempt such as decreasing the working potential and Nafion-treatment (*16*) would overcome this problem.

SUMMARY

This work reports on bioelectrocatalytic detection of histamine, a well-known biomaker for food freshness with a histamine dehydrogenase-based electrode. The amperometric analysis of histamine was operated at +0.2 V (vs. standard hydrogen electrode) using polyvinylimdazole complexed with [osmium(2,2'-dipyridylamine)$_2$Cl] as an electron mediator. This electrode was characterized by a linear range of 2–50 μM.

REFERENCES

1. Frattini, V., and Lionetti, C., (1998) *J. Chromatogr. A 809,* 241–245.
2. Lange, J., Thomas, K., and Wittmann, C., (2002) *J. Chromatogr. B 779,* 229–239.
3. Kutlán, D., Presits, P., and Molnár-Perl, I., (2002) *J. Chromatogr. A 949,* 235–248.
4. Niculescu, M., Frébor, I., Peč, P., Galuszka, P., Mattiasson, B., and Csöregi, E. (2000) *Electroanalysis 12,* 369–375.
5. Iwaki, S., Ogasawara, M., Kurita, R., Niwa, O., Tanizawa, K., Ohashi, Y., and Maeyama, K., (2002) *Anal. Biochem. 304,* 236–243.
6. Loughran, M.G., Hall, J. M., Turner, A. P. R., and Davidson, V. L., (1995) *Biosens. Bioelectr. 10,* 569–576.
7. Zeng, K., Tachikawa, H., Zhu, Z., and Davidson, V. L., (2000) *Anal. Chem. 72,* 2211–2215.
8. Bao, L., Sun, D., Tachikawa, H., and Davidson, V.L. (2002) *Anal. Chem. 74,* 1144–1148.
9. Yamamoto, K., Takagi, K., Kano, K., and Ikeda, T. (2001) *Electroanalysis 13,* 375–379.
10. Siddiqui, J. A., Shoeb, S. M., Takayama, S., Shimizu E., and Yorifuji, T. (2000) *FEMS*

Microbiol. Let. 189,183–187.

11. Sato, T., Horiuchi, T., and Nishimura, I. (2005) *Anal. Biochem. 346*, 320–326.
12. Limburg, J., Mure, M., and Klinman, J. P., (2005) *Archives Biochem. Biophys. 436*, 8–22.
13. Takagi, K., and Shikata, S., (2004) *Analytica Chim. Acta 55*,189–193.
14. Tsujimura, S., Kano, K., and Ikeda, T., (2002) *Chem. Lett. 10*, 1022–1023.
15. Fujieda, N., Tsuse, N., Satoh, A., Ikeda, T., and Kano, K., (2005) *Biosci. Biotech. Biochem. 69*, 2459–2462.
16. Wang, J., and Golden, T. (1989) *Anal. Chem. 61*, 1397–1400.

CONCLUSIONS

The results in this study can be concluded as follows:

CHAPTER 1

The thermodynamic and kinetic analysis of redox behavior of QH-AmDH, and reductive activation and characterization of *s*QH-AmDH are presented. By MCES, the redox potentials of two hemes *c* in QH-AmDH from *P. denitrificans* were evaluated and determined to be 0.149 and 0.235 V, respectively. From kinetic, spectroscopic, and structural aspects, the former value was assigned to heme *c* (b), which is buried in QH-AmDH, and the latter to solvent accessible heme *c* (a). Isolation of CTQ-containing γ subunit allowed the author to observe redox behavior of CTQ spectroelectrochemically. Electrochemical and spectral properties of CTQ were characterized. Its redox potential was determined as 0.065 V at pH 7.0, and depended on pH in the range from 6 to 11. The author discussed electron transfer in QH-AmDH thermodynamically and structurally on the basis of these redox potentials.

The steady-state kinetic parameters of electron transfer reactions from QH-AmDH to two metalloproteins, amicyanin and cytochrome *c* from horse heart were measured electrochemically by using the promoter-modified gold electrodes. The bimolecular rate constants of these reactions were very large and the reactions were so fast, although the physiological electron acceptor of QH-AmDH is cytochrom c_{550}. It appeared that the parameters were independent of the redox potential and isoelectric point of these metalloproteins. The reconstitution of respiratory chains was also performed with these metalloprotein and slurry of cell membrane. The rapid electron flow of respiratory chains, which included inter-protein electron transfer described above, was observed in the experiments.

The unique hemoprotein, of which the spectral properties and subunit structure are very similar to those of QH-AmDH, was slowly activated by substrate amine and immediately by chemical reductants such as dithionite and dithiothreitol. From the activation experiments,

this protein was identified as a silent form of QH-AmDH (*s*QH-AmDH). *s*QH-AmDH was confirmed to have no mature CTQ as juded from its reactivity with hydrazone formation. UV-vis spectrum of γ subunit of *s*QH-AmDH is also unique and distinct clearly from that of QH-AmDH, but is almost identical to that of hydroxylamine adduct of QH-AmDH. This adduct was also activated by amine and dithionite. These results showed that *s*QH-AmDH had CTQ-*6*-oxime as a chromophore.

CHAPTER 2

Biochemical characterization and production in *E. coli* of HmDH were demonstrated. The *hmd* gene, which encodes HmDH from *Nocardioides simplex*, was cloned and sequenced by degenerated- and TAIL-PCR methods. From alignment analysis of amino acid sequence, the sequence of HmDH was closely related to that of TMADH, containing a 6-*S*-cysteinyl-FMN and a 4Fe-4S cluster. These cofactors have been confirmed by chemical analysis. HmDH is very similar to TMADH, but in structural modeling study, a putative substrate-binding cavity of HmDH was quite different from that of trimethylamine dehydrogenase.

The *hmd* gene was also overexpressed in *Escherichia coli*, and the resulting enzyme was purified to homogeneity. The purified recombinant enzyme had the relative activity equal to native enzyme. Interestingly, the recombinant enzyme was completely assembled with not only 4Fe-4S cluster but also 6-*S*-cysteinyl-FMN. Both HmDHs has an ADP in one subunit, although its function remains unknown. Thus, the recombinant enzyme is almost identical with the native enzyme, indicating that recombinant HmDH can safely be used as a substitute for the native enzyme.

Application to histamine sensors of HmDH was also described. Utilization of polyvinylimdazole complexed with [osmium(2,2'-dipyridylamine)$_2$Cl] as an electron mediator allowed the author to detect histamine electrochemically at a low potential of +0.2 V (vs. SHE). Response currents for histamine of this HmDH-based electrode increased linearly to 50 μM. This modified electrode could be successfully applied to determination of histamine in food samples.

ACKNOWLEDGEMENTS

I would like to express my sincere gratitude to Dr. Kenji Kano, Professor of Kyoto University, of his kind guidance and important suggestions during the preparation of this thesis and the course of this work. I would like to express also my heartfelt gratitude to Dr. Tokuji Ikeda, Professor of Fukui Prefectual University, for his generous guidance, invaluable advice, and continuous encouragement. I also thank Dr. Tadaaki Kakutani, Associate Professor of Kyoto University.

I would like to express my appreciation to Dr. Kazuyoshi Takagi, Associate Professor of Ritumeikan University, for his meaningful advices in purification of quinohemoprotein amine dehydrgeonase and histamine dehydrogenase, and midnight support. I show my appreciation to Dr. Michihiko Kataoka, Associate Professor of Kyoto University, for his kind guidance and collaboration on the work of Edman degradation and also to Dr. Takaaki Nishioka, Professor of Kyoto University, Dr. Hideto Miyoshi, Associate Professor of Kyoto University, Dr. Atsushi Ishihara, Instructor of Kyoto University, and Dr. Yozo Okazaki for their important advices and guidance on the work of ultracentrifugation and electron spray ionization mass spectroscopy. I am grateful to Dr. Kazunobu Matsushita, Professor of Yamaguchi University, and Dr. Hirohide Toyama, Associate Professor of Yamaguchi University, for their kind helps and guidances in culture of bacteria and cloning of the gene encoding histamine dehydrogenase. I am also grateful to Dr. Hiroya Yurimoto, Instructor of Kyoto University and Dr. Yoshitaka Ano for technical advices on the work of mini-labo, French press.

Special thanks must extend to members of Kano laboratory, and especially to Mr. Seiya Tsujimura, Instructor of Kyoto University, Dr. Atsuko Satoh, Mr. Noriaki Tsuse, Mr. Akio Ishii, and Ms. Maiko Tsutsumi for their kind support in my laboratory work. Also special thanks to Dr. Hirosuke Tatsumi, Instructor of Fukui Prefectual University, Dr. Shin-ichi Yamazaki, Mr. Atsuhiro Satoh, Ms. Megumi Mori, Mr. Ryuhei Matsumoto, Mr. Yosuke Ito, Mr. Seiya Sakaguchi, Mr. Moriaki Arasaki, Ms. Akiko Nakanishi, Mr. Ryo Nakayama for their advices and helps.

I thank to members of Kihara laboratory and Kakiuchi laboratory, especially to Dr. Sorin Kihara, Professor of Kyoto Institute of Technology, Dr. Takashi Kakiuchi, Professor of Kyoto University, Dr. Kohji Maeda, Associate Professor of Kyoto Institute of Technology, Dr. Masahiro Yamamoto, Associate Professor of Kyoto University, Dr. Yumi Yoshida, Instructor of Institute of Technology, and Dr. Naoya Nishi, Instructor of Kyoto University for their advices, kindness, and encouragenment.

Finally, let me express my greatest thanks to my family: to my father Hatsumi, mother Nobue, and brother Hiromitsu, and to my wife's parents, Yoshirou and Mariko Hirai for their continuous encouragement. Naturally I am deeply grateful for my wife Rieko.

PUBLICATION LIST

Spectroelectrochemical Evaluation of Redox Potentials of Cysteine Tryptophylquinone and Two Hemes *c* in Quinohemoprotein Amine Dehydrogenase from *Paracoccus denitrificans*
Fujieda, N., Mori, M., Kano K., and Ikeda, T.
(2002) *Biochemistry*, *41* (46), 13736 - 13743.

Redox Properties of Quinohemoprotein Amine Dehydrogenase from *Paracoccus denitrificans*
Fujieda, N., Mori, M., Kano, K. and Ikeda, T.
(2003) *Biochim. Biophys. Acta*, *1647* (1/2), 289 - 296.

6-*S*-Cysteinyl Flavin Mononucleotide-Containing Histamine Dehydrogenase from *Nocardioides simplex*: Molecular Cloning, Sequencing, Overexpression and Characterization of Redox Centers of Enzyme
Fujieda, N., Satoh, A., Tsuse, N., Kano, K., and Ikeda, T.
(2004) *Biochemistry*, *43* (33), 10800-10808.

Production of Completely Flavinylated Histamine Dehydrogenase, Unique Covalently Bound Flavin and Iron-Sulfur Cluster Containing Enzyme, of *Nocardioides simplex* in *Escherichia coli* and Its Properties
Fujieda, N., Tsuse, N., Satoh, A., Ikeda, T., and Kano, K.
(2005) *Biosci. Biotech. Biochem.*, *69* (12), 2459-2462.

Reductive Activation and Characterization of Silent Form Quinohemoprotein Amine Dehydrogenase from *Paracoccus denitrificans*
Mori, M., Fujieda, N., Kano, K., and Ikeda, T. in preparation.

Bioelectrocatalytic Detection of Histamine with Histamine Dehydrogenase-Based Electrode
Fujieda, N., Tsujimura, S., and Kano, K. in preparation.